WORKSHOP ON MOUNTAIN BELTS ON VENUS AND EARTH

San Juan Capistrano, California
January 13-15, 1992

Sponsored by

Lunar and Planetary Institute
San Juan Capistrano Research Institute
NASA Johnson Space Center

WORKSHOP ON

MOUNTAIN BELTS ON VENUS AND EARTH

San Juan Capistrano, California

January 13-15, 1992

Sponsored by

Lunar and Planetary Institute
San Juan Capistrano Research Institute
NASA Johnson Space Center

Compiled in 1991 by

Lunar and Planetary Institute
3303 NASA Road 1
Houston TX 77058-4399

The Lunar and Planetary Institute is operated by the Universities Space Research Association under Contract No. NASW-4574 with the National Aeronautics and Space Administration.

PREFACE

This volume contains abstracts that have been accepted for the Workshop on Mountain Belts on Venus and Earth, January 13-15, 1992, in San Juan Capistrano, California. Co-conveners Sean Solomon (Massachusetts Institute of Technology) and John Suppe (Princeton University) were responsible for the program.

Logistics and administrative support were provided by the Program Services Department staff at the Lunar and Planetary Institute. This abstract volume was prepared by the Publications Services Department staff at the Lunar and Planetary Institute.

CONTENTS

Terrestrial Mountain Belts and Venusian Plateau-shaped Highlands as Manifestations of Mantle Downwelling
D. L. Bindschadler 1

Rheologic Controls on Lithospheric Extension
W. R. Buck and J. R. Hopper 4

Sustainability of Subduction in the Venus Environment
J. D. Burt 7

Characteristics of Fold-and-Thrust Belts on Venus
C. Connors and J. Suppe 10

Critical-Taper Model of Fold-and-Thrust Belts on Earth and Venus
F. A. Dahlen, J. Suppe, C. Connors and E. Price 13

Imaged Fracture Set Orientations and Venus Fault Mechanics
D. M. Davis and A. E. Small 16

The Southern and Central Appalachians and the Growth of SE North America, Applications to Tectonically Active Planets
R. D. Hatcher Jr. and P. J. Lemiszki 18

Maxwell and the Andes: Similarities and Contrasts
W. M. Kaula, A. Lenardic, and D. L. Bindschadler 21

Rheology of the Crust and Upper Mantle of Venus: Constraints Imposed by Laboratory Experiments
D. L. Kohlstedt 24

The Thermal Structure of Mountain Belts on Venus: Volcanism and Mantle Heat Flow in the Freyja Montes Region
N. Namiki and S. C. Solomon 25

Geophysical Constraints on Venusian Mountain Belts
R. J. Phillips and R. E. Grimm 28

Investigations of the Surface of Venus Using Magellan Data
R. S. Saunders 31

Coupling Between Mantle Convection and Crustal Deformation on Venus
M. Simons, S. C. Solomon, and B. H. Hager 32

Gravitational Spreading of Plateaus and Mountain Belts on Venus
S. E. Smrekar and S. C. Solomon 35

Venus: An Overview of Global and Regional Tectonics
S. C. Solomon 38

The Deformation Belts of Lavinia Planitia
S. W. Squyres, D. G. Jankowski, M. Simons, S. C. Solomon, B. H. Hager, and G. E. McGill 41

Corona Annuli: Plume-Related Mountain Belt Formation on Venus
E. R. Stofan, D. L. Bindschadler, and G. Schubert 44

Tectonic Settings of the Mountain Belts of Venus
J. Suppe and C. Connors 46

Finite Amplitude, Non-Newtonian Folding of the Lithosphere on Venus and Earth
M. T. Zuber and E. M. Parmentier 49

TERRESTRIAL MOUNTAIN BELTS AND VENUSIAN PLATEAU-SHAPED HIGHLANDS AS MANIFESTATIONS OF MANTLE DOWNWELLING.

D.L. Bindschadler, Dept. Earth and Space Sciences, UCLA, Los Angeles, CA 90024.

Mountain belts are the predominant surface expression of intensive compressional deformation on the surface of Earth. Taken together, both actively deforming (e.g., the Andes, Tibet) and remnant mountain ranges (e.g., the Appalachians) constitute a significant fraction of the surface area of the Earth. Terrestrial mountain belts are formed along convergent plate margins by a combination of compressional deformation and crustal thickening and intrusive and extrusive magmatic activity. Convergence and associated deformation are thought to be driven primarily by the subduction of oceanic lithosphere, which is the Earth's primary mode of mantle downwelling.

The predominant surface expressions of intensive compressional deformation on Venus are plateau-shaped highlands [1]. These are steep-sided, topographically rugged regions whose surfaces are dominated by complex ridged (or *tessera*) terrain. They constitute a significant fraction of the surface area of Venus (~5-10%) and are distinct from volcanic rises such as Atla and Beta Regiones [1], which are thought to be due to large mantle upwellings or plumes. The formation of these plateau-shaped highlands and associated complex ridged terrain appears to be a manifestation of downwelling within the mantle of Venus [2,1]. I review characteristics of these plateau-shaped highlands and current understanding of their mode of formation, then note some of the questions which may help us to understand the differences and similarities in the formation of compressional highlands on Earth and Venus.

While mountain belts have been recognized on Venus, they constitute only a tiny fraction of the surface (~0.35%) [3] and are restricted to a geographically small region. Ridge belts are also widely accepted as compressional features, but their relatively low relief (<1 km) and limited extent (~100 km across) suggests they are due to modest amounts of compressional deformation. A third type of compressional terrain, complex ridged (tessera) terrain, was recognized on the basis of Venera 15/16 radar images [4, 5]. Magellan radar images have revealed that complex ridged terrain is widely distributed on Venus and is the dominant highland terrain [1]. It dominates Ishtar Terra, Tellus Regio, Laima Tessera, and numerous smaller upland regions in northern Venus [6]. Magellan images show that it dominates Ovda and Thetis Regiones and the rest of westernmost Aphrodite Terra, Alpha Regio, and Phoebe Regio, as well as covering broad areas within and near Beta Regio, and in Lada Terra [7,1].

Analysis of Venera images of Tellus Regio and Fortuna Tessera [5], detailed examination of Magellan images of Alpha Regio [8], and preliminary examination of Magellan images for most plateau-shaped highlands [9,1] all indicate that compressional ridges are the oldest discernable structures present within these regions and are commonly superposed by extensive extensional structures. While hotspot and crustal spreading models have been suggested for the formation of plateau-shaped highlands and complex ridged terrain [10,11], such models fail to explain several key characteristics of these regions. The single most important of these is the

MANTLE DOWNWELLINGS
Bindschadler, D.L.

presence of margin-parallel compressional structures. These structures are commonly found at the highest elevations within a given highland; the highest elevations are not in the center of a highland, but near the boundary between the highland's complex ridged terrain and the lowland plains. Such a correlation of structure and topography is inconsistent with both hotspot and spreading models, but is predicted for highlands formed over mantle downwellings [12,13]

Mantle downwelling leads to the formation of a plateau-shaped highland by pulling crustal material toward a region of downflow. Deformation is driven by the horizontal pressure gradients responsible for the downflow and by horizontal shear stresses transmitted across the crust-mantle boundary [2]. Mantle downwelling initially causes subsidence and the formation of a circular or linear lowland (e.g., Atalanta or Sedna Planitiae). Continued downwelling leads to crustal thickening and attendant uplift and deformation on timescales of a few hundred million years or less for likely values of crustal and mantle viscosity [2,13]. During much of this uplift time, deformation is dominated by margin-parallel compression [13,14]. As downwelling continues, deformation within the interior of such a plateau can become extensional [2,12]; once it ceases, the region of thick crust is likely to spread under its own weight, causing both decreases in elevation and extensional deformation. These latter processes may explain the presence of young extensional structures within the plateau-shaped highlands.

Even if no terrestrial-like subduction occurs on Venus, convection necessitates some form of downflow. This downflow represents a significant driving force for tectonic deformation. Models of convection in uniform-viscosity spherical shells [15] indicate that the highest convective velocities (and thus, the largest potential convective stresses) for a largely-internally heated mantle are associated with regions of downwelling. Other considerations suggest that conditions necessary for the formation of plateau-shaped highlands by mantle downwelling are present on Venus. These include the presence of a ductile lower crust and viscous coupling of mantle convective flow into the crust [2]. These conditions are provided by the high surface temperature on Venus, which allows for ductile behavior of crustal materials at depths of only a few kilometers on Venus, and the apparent lack of an asthenosphere or low-viscosity layer on Venus [16], which causes stresses associated with mantle flow to be more strongly coupled into the lower crust [2]. Given such conditions, lower crustal material can be pulled toward coldspots (downwellings) by the horizontal pressure gradients due to downflow and by horizontal shear stresses transmitted across the crust-mantle boundary.

Mantle downwellings occur on both Earth and Venus but apparently are manifested somewhat differently. The lack of water on Venus is suggested to be the root cause of Venus' lack of an asthenosphere [17]. Such a lack not only tends to favor downwelling-driven crustal thickening as described above, but also to inhibit the formation of separate lithospheric plates [1]. The high surface temperature leads to a less brittle, more viscous lithospheric rheology [1]. These differences may explain some of the differences between terrestrial mountain belts and venusian plateau-shaped highlands, such as the axisymmetric to irregular equi-dimensional shape of most plateau-shaped highlands and the extreme complexity and apparently more-diffuse nature of the deformation observed on Venus.

In general, little detailed comparison between the major compressional highlands on Earth and Venus has been done and numerous points of comparison between terrestrial mountain belts and venusian plateau-shaped highlands remain to be examined. What role does erosion play in terrestrial mountain-building and how is the formation of compressional highlands on Venus affected its near-absence? How do the structural geologies of plateau-shaped highlands on Venus compare with topographically similar regions on Earth such as the Altiplano or the Tibetan Plateau? Extensional deformation is evident in venusian plateau-shaped highlands. How does it compare with the evident extension within such regions as the Andes, Tibetan Plateau, and Basin and Range?

REFERENCES

[1] Bindschadler, D.L., G. Schubert, W.M. Kaula, Coldspots and hotspots: Global tectonics and mantle dynamics of Venus, *J. Geophys. Res.*, submitted, 1992.

[2] Bindschadler, D.L. and E.M. Parmentier, *J. Geophys. Res., 95,* 21,329-21,344, 1990.

[3] Bindschadler, D.L., and J.W. Head, *Icarus, 77,* 3-20, 1989.

[4] Basilevsky, A.T., Pronin, A.A., Ronca, L.B., Kryuchkov, V.P., Sukhanov, A.L., *Proc. Sixteenth Lunar Planet Sci. Conf., Part 2, J. Geophys. Res., 91,* D399-D411, 1986.

[5] Bindschadler, D.L., and J.W. Head, *J. Geophys. Res., 96,* 5889-5907, 1991.

[6] Barsukov, V.L., A.T. Basilevsky, G.A. Burba, N.N. Bobina, V.P. Kryuchkov, et al., *Proc. Sixteenth Lunar Planet Sci. Conf., Part 2, J. Geophys. Res., 91,* D378-D398, 1986.

[7] Bindschadler, D.L., M.A. Kreslavsky, M.A. Ivanov, J.W. Head, A.T. Basilevsky, and Yu.G. Shkuratov, *Geophys. Res. Lett., 17,* 171-174, 1990.

[8] Bindschadler, D.L., A. de Charon, K.K. Beratan, S.E. Smrekar, and J.W. Head, Magellan observations of Alpha Regio: Implications for the formation of complex ridged terrains on Venus, *J. Geophys. Res.*, submitted, 1992.

[9] Saunders, R.S., J.W. Head, R.J. Phillips, S.C. Solomon, R. Herrick, R.E. Grimm, and E.R. Stofan, *Lunar Planet. Sci. XXII,* 1169-1170, 1991

[10] Head, J.W., and L.S. Crumpler, *Nature, 346,* 525-533, 1990.

[11] Herrick, R.R., and R.J. Phillips, *Geophys. Res. Lett., 17,* 2129-2132, 1990.

[12] Bindschadler, D.L., G. Schubert, and W.M. Kaula, *Geophys. Res. Lett., 17,* 1345-1348, 1990.

[13] Lenardic, A., W.M. Kaula, and D.L. Bindschadler, *Geophys. Res. Lett.*, in press, 1991.

[14] Grimm, R.E., and R.J. Phillips, *J. Geophys. Res, 96,* 8305-8324, 1991.

[15] Bercovici, D., G. Schubert, and G.A. Glatzmaier, *Science, 244,* 950-955, 1989; Bercovici, D., G. Schubert, and G.A. Glatzmaier, *Geophys. Res. Lett., 16,* 617-620, 1989; Schubert, G., D. Bercovici, and G.A. Glatzmaier, *J. Geophys. Res., 95,* 14105-14129, 1990.

[16] Kiefer, W.S., M.A. Richards, B.H. Hager, and B.G. Bills, *Geophys. Res. Lett., 13,* 14-17, 1986.

[17] Kaula, W.M., *Science, 247,* 1191-1196, 1990.

RHEOLOGIC CONTROLS ON LITHOSPHERIC EXTENSION, W. Roger Buck and John R. Hopper, Lamont-Doherty Geological Observatory of Columbia University, Palisades NY 10964.

There are two obvious differences in the environment of Venus and Earth which may have important effects on the style of extension on those planets. One difference is that the lithosphere on Venus may be much drier than the lithosphere of Earth. A second difference is that the surface temperature on Venus is about 450°C hotter than on Earth. We have investigated both of these differences in two studies which are described here.

To look at the problem of different surface temperatures a simplified model of continental extension including lower crustal flow is developed. The model employs the thin sheet approximation in estimating lithospheric yield strength and gravitational buoyancy forces arising from lateral variations in crustal thickness and temperature. The effect of advection and diffusion of heat on the temperature structure and yield strength of the extending region is calculated. The viscosity of the lower crust, which controls its rate of flow, is estimated in a manner consistent with the yield strength calculation. The change in the force required to extend the lithosphere is calculated after a finite amount of extension. When this force increases, the zone of extension is assumed to widen; when it decreases, the extension remains localized. The model predicts three distinct modes of extension depending on the model crustal thickness, heat flow, and strain rate. The modes are (1) core complex mode (concentrated upper crustal extension with lower crustal thinning over a broad area and any mantle lithosphere extending in a local area), (2) wide rift mode (uniform crustal and mantle lithospheric thinning over a width greater than the lithospheric thickness), and (3) narrow rift mode (concentrated crustal and mantle lithospheric extension). Figure 1 shows the different predicted conditions of crustal thickness and heat flow for Venus and Earth with the only difference in the models being the surface temperatures.

The second problem concerns the tectonic force needed for rifts to develop. In the first problem, we assumed that whatever tectonic force needed for extension could exist. This is unlikely to be true. The tectonic force driving the extension of East Africa, for example is likely to be only about 2×10^{12} Nt/ m (roughly equal to the ridge push force). This would be insufficient to cause extension of cold lithosphere given the rheology assumed above which uses a power law relation of n=3 for the plastic portions of the lithosphere. In this case, the forces required to cause extension at geologically reasonable strain rates would have to be greater than 20×10^{12} Nt/ m. One way around this is if grain boundary diffusion mechanisms such as pressure solution are important in the mantle. These flow laws have a power law exponent n≈1 and low activation energies which serve to reduce the thermal dependence of strength while increasing the strain rate dependence. Thus, if something analogous to pressure solution can operate in the Earth's upper mantle, it is possible to have a weak mantle in cold areas that are straining slowly.

We have calculated the strength and thermal state of the lithosphere through time assuming that a constant tectonic force is available to drive extension. Initially, a power law n≈1 rheology dominates the mantle strength. As the lithosphere thins, the strain rate which maintains a constant lithospheric strength increases. Eventually, a power law n≈3 rheology can come to dominate. Our results show that as strain rates increase past 5×10^{-15}, extension accelerates rapidly, implying the onset of lithospheric break-up. We calculated the amount of time it takes for strain rates to reach this point for a given applied tectonic force for both a power law n≈3 rheology and an n≈1 rheology (figure 2). For the

former case, the tectonic forces required to cause rapid rifting in a geologically reasonable amount of time are on the order of 20 x 10^{12} Nt/ m while for the latter case tectonic forces of about 10 x 10^{12} Nt/ m can cause break-up within a reasonable amount of time.

Whether the Earth's mantle is wet or dry is largely unknown; however, the presence of water may be essential for allowing n≈1 rheologies to operate. Thus a wet mantle on Earth could serve to greatly weaken the lithosphere allowing for the initiation of rifting at slow strain rates. If insufficient water is available in the mantle of Venus for this mechanism, then the strength of the mantle there may be too great for rifting to initiate in the same manner as it does on the Earth.

The model is very simple because we are only calculating the effects of bulk deformation through grain boundary diffusion processes. A more realistic way for grain boundary diffusion mechanisms to weaken the lithosphere may be through the creation of shear zones where the strain is highly localized and metamorphic processes cause a grain size reduction that greatly enhances the mechanism. Our model is therefore a preliminary study of grain boundary diffusion effects on the tectonic force required to make rifts.

The tectonic force available for driving extension is limited, though we do not have an exact estimate of the level of that force. We speculate that in an environment where the lithosphere is dry the only way that available tectonic forces can lead to extension is where the lithosphere is thinner than the average value. Rifts cannot propagate into regions that are moderately cold. On the other hand, if the lithosphere is wet then rifts can propagate into cold regions and then localized lithospheric thinning further reduces the strength of the area of the rift. This propagation of rifts through areas of cold crust may be a necessary condition for the development of plate tectonics.

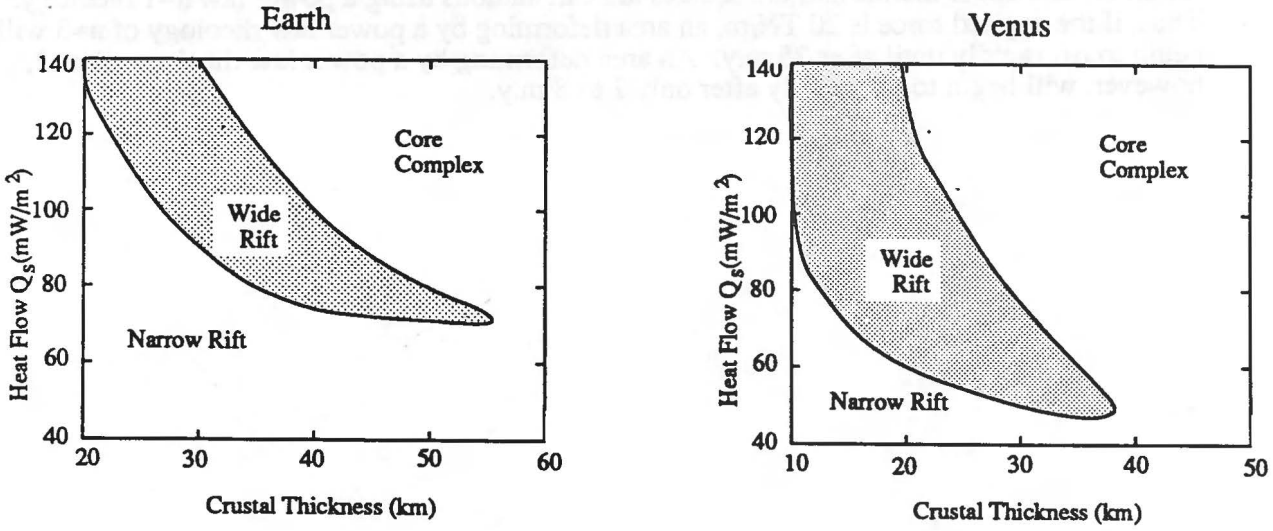

Figure 1. Mode boundaries in surface heat flow-crustal thickness space for Earth and Venus. Note that the ranges for the horizontal scales are different. The only difference in the calculations is that the surface temperatures are different by 450°C.

Rheologic Controls on Lithospheric Extension
Buck, W.R. and Hopper, J.R.

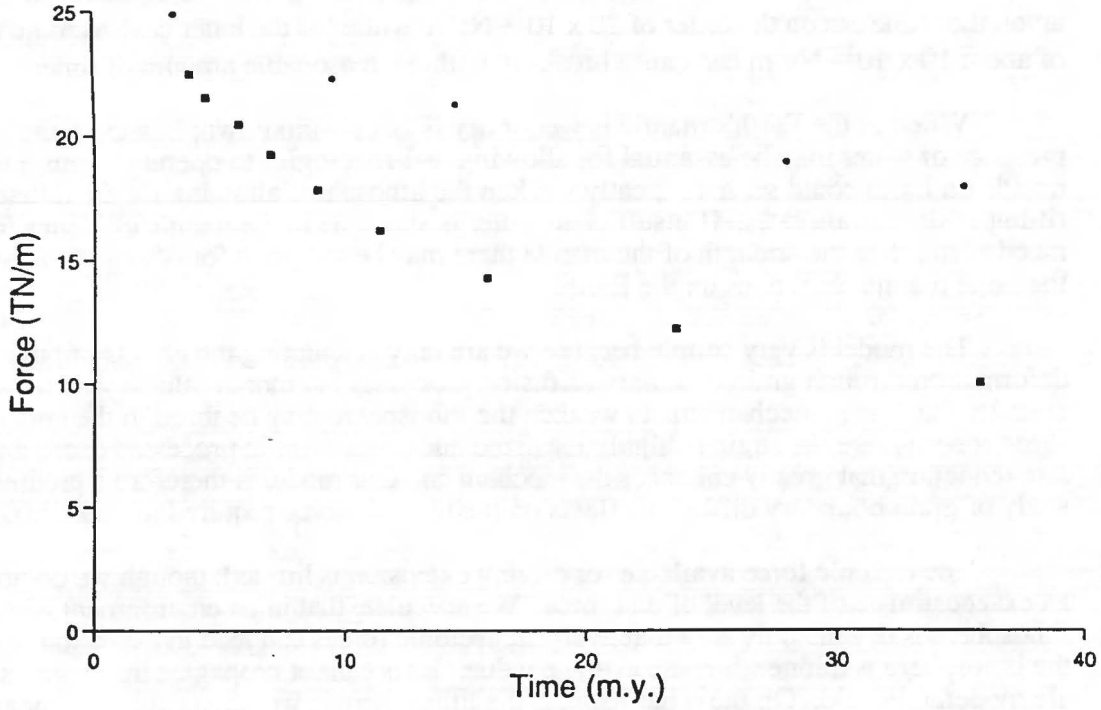

Figure 2. Plot of the time required for the strain rate to reach $5x10^{-15}$ 1/sec for a given applied tectonic force (in 10^{12} N/m) assuming that the strain rate during extension changes such that the applied force remains constant. The circles represent calculations for a power law n≈3 rheology for an olivine upper mantle and the squares are calculations using a power law n≈1 rheology. Thus, if the applied force is 20 TN/m, an area deforming by a power law rheology of n≈3 will not begin to rift rapidly until after 25 m.y. An area deforming by a power law rheology of n≈1, however, will begin to rift rapidly after only 7 to 8 m.y.

SUSTAINABILITY OF SUBDUCTION IN THE VENUS ENVIRONMENT:

J.D. Burt, Department of Geological Sciences, Brown University, Providence, R.I., 02912

Introduction: In evaluating the role of plate tectonics and crustal recycling in the heat transport of Venus enhanced surface temperatures and a thinner lithosphere relative to Earth's have been sited as leading to increased lithospheric buoyancy. This would then limit (1), or prevent (2) subduction on Venus. The dependence of lithospheric buoyancy on factors poorly constrained for Venus (including: crustal thickness, the partitioning of heat loss between plate recycling and other modes of heat transport, and the location of the mantle residuum depleted during crustal formation (3)) and the subduction of terrestrial oceanic lithosphere of a wide range of ages and buoyancies (3), implies that subduction cannot be dismissed readily for Venus (3). Further, subduction and crustal underthrusting have been proposed as contributing to the formation of a number of features on Venus. For example, Freyja Montes, a linear mountain belt in the northern hemisphere of Venus, has been interpreted to be an orogenic belt (4) and a zone of convergence and underthrusting of the north polar plains beneath Ishtar Terra, with consequent crustal thickening and possible subduction (5). Danu Montes, also a linear mountain belt on Venus, has been interpreted to represent the location of crustal underthrusting (6). Further investigation of the possibility of subduction on Venus is thus warranted.

This study evaluates the maintenance of subduction once it is initiated. It is assumed that subduction, once started, continues as long as the angle of subduction does not decrease to near zero. Thus a driving force is assumed sufficient to maintain underthrusting of the slab. Thermal changes in slabs subducting into a mantle having a range of initial geotherms are used to predict density changes and, thus, the overall buoyancy of the slab. Buoyancy effects on subductibility are then evaluated using a model for subduction-induced mantle flow. Mantle flow applies torques to the slab and act in concert with or opposition to buoyancy torques to change the angle of subduction.

Subduction Model: The modelling assumes slabs, having a thickness set by the 750°C isotherm (7), subduct at a 45 degree angle into the mantle. A set of initial geotherms were calculated, using the instantaneous cooling of a semi-infinite half space, to match surface thermal gradients of 10°C/km, 15°C/km, and 25°C/km (8).

The mantle and slab materials are assumed to be basaltic (material properties insignificantly differing between basalt and peridotite in terms of heat conduction). Slabs heat via conduction, crustal radioactivity, changes of phase, and adiabatic compression of the slab material. Phase changes involving the conversion of basalt to eclogite at depths of 60 to 160 km and then enstatite to forsterite plus stishovite between 260 and 360 km generate 0.13×10^{-5} ergs/cm^3 s and 0.36×10^{-5} ergs/cm^3 s respectively (9). The assumed slab radiogenic heat production is 4.0×10^{-7} ergs/gm s. Radioactivity in the mantle was considered negligible and ignored. Adiabatic compression adds 0.5°C per kilometer of depth. Subduction rates ranged from 5 mm/yr, equalling the rate derived from modelling of crustal spreading on Venus (10), to 100 mm/yr.

The thermal evolution of the slab is followed using a finite difference technique (9 and 11). The model region measures approximately 800 km horizontally by 400 km deep. Processing ends at the point where slab tips reach a 300 km depth, implying time intervals of 10 m.y. to 100 m.y.

Slab density changes derive from the thermal results through calculation of the thermal expansion (volumetric coefficient of thermal expansion: $\alpha_V = 3 \times 10^{-5}$ /°K (12)) and the effects of pressure (isothermal compressibility: $\beta = 1 \times 10^{-3}$/kb (12))on an initial density distribution set for zero pressure and temperature. The assumed initial density structure includes a 15 km basaltic crust (10), having a density of 3.0 gm/cm^3 ; an approximately 40 km thick depleted mantle zone of density 3.295 gm/cm^3 ; and underlying undepleted mantle, density=3.36 gm/cm^3 . Density changes due to the phase transitions are also included. Results are produced in the form of contour plots of density throughout the model region in both the slab and mantle.

Results: Figure 1 shows a typical result of the density processing. Density contours (contours have a 0.025gm/cm^3 spacing) within the mantle and slab clearly delineate the slab. In this case, for the 15°C/km initial geotherm and a subduction rate of 5 km/my, the slab densities in the region above the basalt-eclogite phase transition are lower than their mantle surroundings (The phase change is set for the density analysis at around 110 km depth). In other cases, such as with the 10°C/km geotherm and a subduction rate of 100 km/my, slab densities in the zone above this phase change are greater than those in the adjacent mantle (figure 2). Below the basalt-eclogite phase change densities in the slab exceed those in the neighboring mantle in all cases of geotherm and subduction rate.

Discussion: Qualitatively, subduction, once initiated, is likely to be enhanced by the generally negative buoyancy found for the slabs. Only in the shallow zone above the basalt-eclogite phase transition is any hindrance to subduction encountered, and that only in the steeper geotherms. There, positive buoyancy would tend to oppose subduction. In contrast, for the 10°C/km geotherm, negative buoyancy in this shallow region would abet subduction.

An evaluation of the effects of buoyancy on subduction was made using a model for mantle flow induced by the motion of the subducted slab (12). This flow creates pressures on the slab surfaces which apply a torque to the body of the slab. The buoyancy body forces may also be resolved into a torque on the slab, and both torques are here taken to act on the slab as a rigid unit about its junction with the surface. Buoyancy torques are listed in Table 1 for a set of four subduction rates. The torques resulting from mantle flow are given in Table 2 for a range of subduction angles and a subduction rate of 100 km/my as an example providing the most extreme torques.

SUSTAINABILITY OF SUBDUCTION: Burt, J.D.

Generally, the flow torques are small and negative for subduction angles over about 25 degrees, and become positive and increase with decreasing angle below 25 degrees. Two slab lengths are given in each table. The longer, 400 km, is the limit of the slab length set in the subduction modelling, while the shorter, 110 km, reflects only the slab above the basalt-eclogite phase change.

Torques having positive values tend to increase the subduction angle in these examples. For all cases of subduction rate and geotherm the 400 km long slab buoyancy torques are positive and large. They overwhelm flow torques except for the 25°C/km geotherm near a subduction angle of 25 degrees. Thus, a slab reaching the 400 km depth at an angle of 45 degrees would tend to continue subducting, at a steeper dip, due to its negative buoyancy.

For the 110 km length slabs and the two steeper geotherms, subduction angles would tend to decrease. However, this decrease would cease between 20 and 25 degrees subduction angle where positive flow torques would balance negative buoyancy torques. A slab subducting into mantle having the 10°C/km geotherm is unique in tending to increase its subduction angle for both the shallow and deep slabs. This is due to the negative buoyancy persisting throughout the length of the slab for this geotherm.

These results indicate that positive lithospheric buoyancy, as modelled here, is not sufficient to prevent subduction on Venus. Assuming subduction is driven by means other than slab pull, positively buoyant slabs, even dipping initially at a shallow angle, may be expected to increase their dip due to mantle flow pressures. Mantle flow torques appear sufficient to force these slabs to descend at an angle sufficient to bring it through the basalt-eclogite phase transition, as long as the outside driving force overcomes the buoyancy as well. Shallowly dipping slabs may be expected to heat slowly and their density would increase as the slab moves through the basalt-eclogite phase change. Further, at least within the accuracy of the mantle flow model, once shallow subduction is initiated mantle flow pressures act to increase the angle of subduction to around 25 degrees even when the slab is somewhat positively buoyant.

References: 1)Phillips, R.J. and Malin, M.C., (1982), in *Venus*, Hunten, D.M., et al. eds., U. AZ Press, Tucson, p.159-214. 2)Anderson, D.L., (1981), *Geophys. Res. Lett., 8*, p.309-311. 3)Solomon, S.C., and Head, J.W., (1982), *J. Geophys. Res., 87, B11*, p.9236-9246. 4)Crumpler, L.S., Head,J.W., and Campbell,D.B., (1986), *Geology, 14*, p.1031-1034. 5)Head, J.W., (1990), *Geology, 18*, p.99-102. 6) Head, J.W., and Burt, J.D. (1990), *LPSC XXI*, p.481. 7)Hoffman, P.F. and Ranalli, G.,(1988), *Geophys. Res. Lett., 10*, p.1077-1080. 8)Hess, P.C. and Head,J.W., (1989), *Abstracts of the 28th International Geological Congress*, p.2-55. 9)Minear, J.W. and Toksoz, M.N., (1970),*J. Geophys. Res., 75*, no.8, p.1397-1419. 10)Sotin, C., Senske, D.A., Head, J.W., and Parmentier, E.M.,(1989), *Earth and Plan. Sci. Lettr., 95*, p. 321-333. 11)Gerald, C.F., (1978), *Applied Numerical Analysis, 2nd ed.*, Addison-Wesley, Reading, MA. 12)Turcotte, D.L. and Schubert, G., (1982), *Geodynamics: Applications of Continuum Physics to Geological Problems*, J. Wiley & Sons, New York, 450 p.

Figure 1. Density distribution in subducted slab and surrounding mantle for 15°/km initial surface geotherm and 5km/my subduction rate.

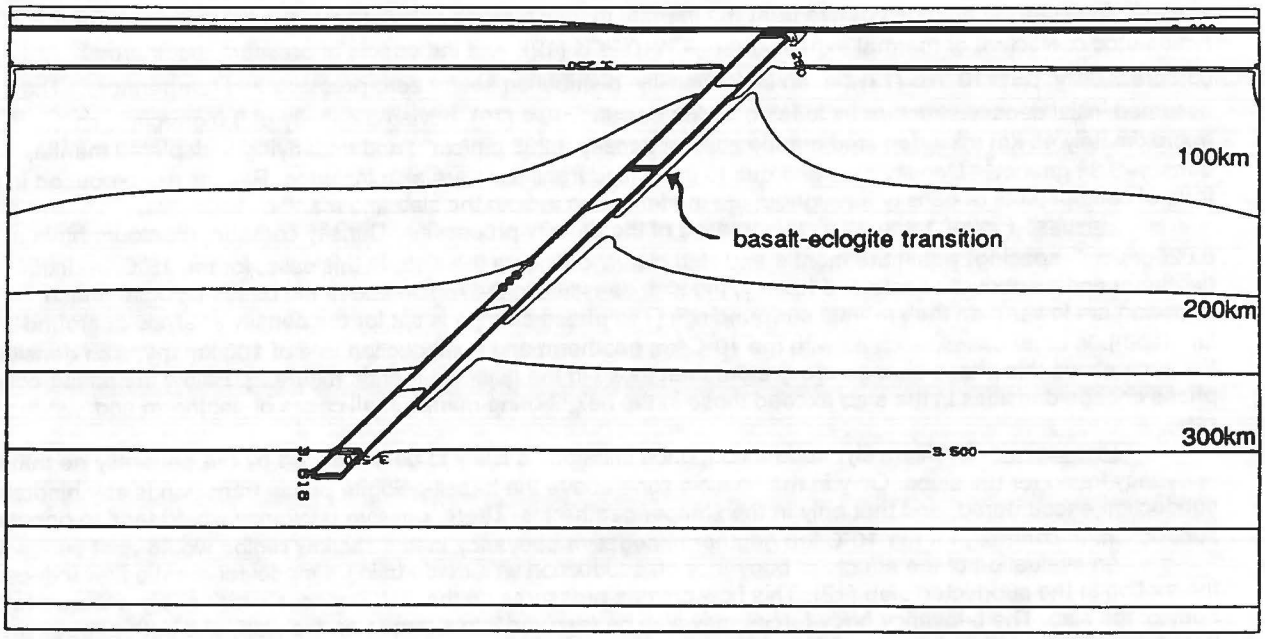

SUSTAINABILITY OF SUBDUCTION: Burt, J.D.

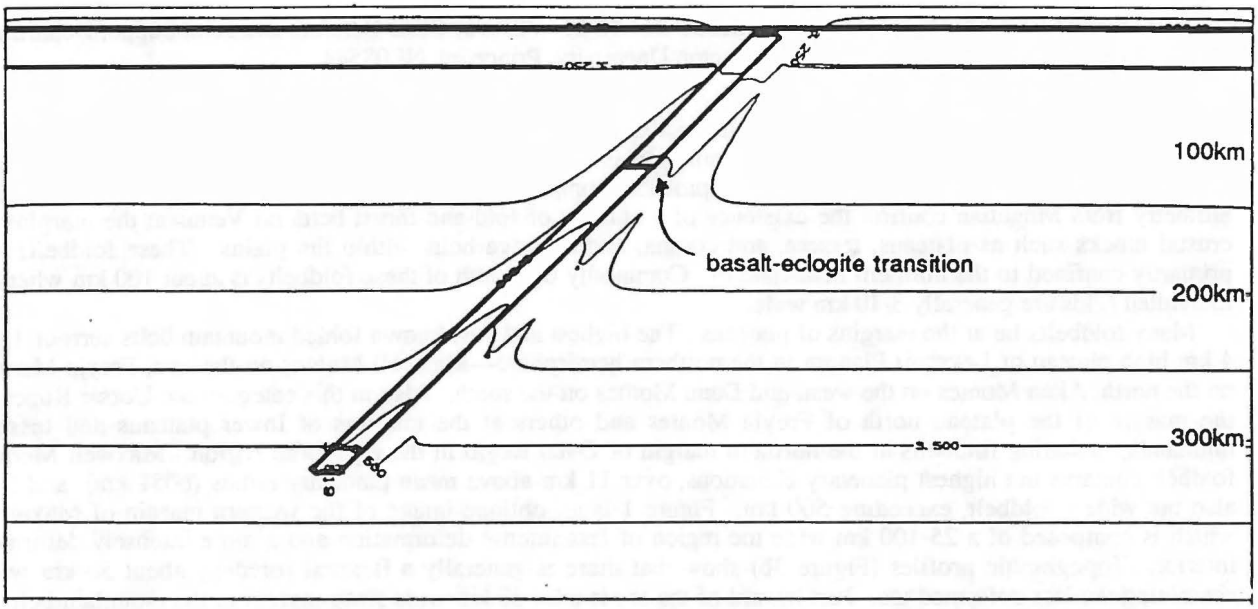

Figure 2. Density distribution in subducted slab and surrounding mantle for 10°/km initial surface geotherm and 100km/my subduction rate.

Table 1: Torques due to slab buoyancy.

		buoyancy torque (Nm)	
geotherm(°C/km)	subd. rate (km/my)	400 km slab	110 km slab
25	100	8.2×10^{20}	-1.4×10^{20}
25	50	7.9×10^{20}	-1.4×10^{20}
25	25	7.8×10^{20}	-1.4×10^{20}
25	5	7.6×10^{20}	-1.5×10^{20}
15	100	1.5×10^{21}	-2.1×10^{20}
15	50	1.4×10^{21}	-2.2×10^{20}
15	25	1.4×10^{21}	-2.2×10^{20}
15	5	1.3×10^{21}	-2.4×10^{20}
10	100	3.7×10^{21}	1.7×10^{20}
10	50	3.5×10^{21}	1.6×10^{20}
10	25	3.5×10^{21}	1.6×10^{20}
10	5	3.3×10^{21}	1.3×10^{20}

Table 2: Torques due to induced mantle flow.

	flow-induced torque	
subduction angle	400 km slab	110 km slab
5	1.2×10^{21}	4.0×10^{20}
10	4.1×10^{20}	1.3×10^{20}
15	2.9×10^{20}	9.4×10^{19}
20	3.9×10^{20}	1.3×10^{20}
25	-5.5×10^{20}	-1.8×10^{20}
30	-9.0×10^{19}	-2.9×10^{19}
35	-3.7×10^{19}	-1.2×10^{19}
40	-2.0×10^{19}	-6.4×10^{18}
45	-1.2×10^{19}	-3.8×10^{18}
50	-7.6×10^{18}	-2.5×10^{18}
55	-5.3×10^{18}	-1.7×10^{18}
60	-4.0×10^{18}	-1.3×10^{18}
65	-3.2×10^{18}	-1.0×10^{18}
70	-2.7×10^{18}	-8.9×10^{17}

CHARACTERISTICS OF FOLD-AND-THRUST BELTS ON VENUS; Chris Connors and John Suppe, Department of Geological and Geophysical Sciences, Princeton University, Princeton, NJ 08544

The presence of compressive mountain belts on Venus could be inferred with substantial certainty based on pre-Magellan data. Radar images and altimetry from Pioneer-Venus[1], Earth-based Arecibo[2], and Venera 15-16[3] have all shown surface features of compressional or probable compressional origin. High-resolution radar imagery and altimetry from Magellan confirm the existence of a number of fold-and-thrust belts on Venus at the margins of crustal blocks such as plateaus, tessera, and corona, and as ridge belts within the plains. These foldbelts are primarily confined to the northern hemisphere[4]. Commonly the width of these foldbelts is about 100 km whereas individual folds are generally 3-10 km wide.

Many foldbelts lie at the margins of plateaus. The highest and best known folded mountain belts surround the 4 km high plateau of Lakshmi Planum in the northern hemisphere—Maxwell Montes on the east, Freyja Montes on the north, Akna Montes on the west, and Danu Montes on the south. Also in this category are Uorsar Rupes at the margin of the plateau north of Freyja Montes and others at the margins of lower plateaus and tessera highlands, including foldbelts at the northern margin of Ovda Regio in the equatorial region. Maxwell Montes foldbelt contains the highest planetary elevations, over 11 km above mean planetary radius (6051 km), and it is also the widest foldbelt, exceeding 500 km. Figure 1 is an oblique image of the western margin of Maxwell, which is composed of a 25-100 km wide toe region of less intense deformation and a more intensely deformed interior. Topographic profiles (Figure 3b) show that there is generally a flexural foredeep about 50 km wide containing the less deformed toe. Just inward of the toe is a 20-30 km wide steep margin to the mountain belt, in which elevations rise about 6 km before a high, deformed plateau is reached. These features of western Maxwell appear in many other foldbelts: *a flexural foredeep, a less deformed toe of low surface slope* (±1°), *a narrow zone of steep slopes* (as high as 10-15°), and *a relatively flat top.*

A number of foldbelts appear at the margins of polydeformed tessera plateaus. The 50 km wide Uorsar Rupes foldbelt north of Lakshmi Planum (Figure 3a) shows a 100 km wide foredeep generally filled with lava, a 30 km wide toe, a 15-20 km wide steep zone and a broad relatively flat crestal massif. The relief of Uorsar from toe to crest is slightly less than 3 km. The interior crestal massifs do not show the folded character displayed by Maxwell; indeed, they appear more like tessera.

Foldbelts are also found at the margin of some larger deformed corona, including Artemis Chasma south of Aphrodite Terra. This 200 km wide and 1500 km long foldbelt lies within an enormous foredeep-like trough between the corona and a great outer flexural high. The structure of the 50 km wide toe of Artemis is particularly interesting because of the well-imaged flat-topped anticlines (Figure 2). The frontal folds display a remarkably constant shape both for individual folds along strike and between adjacent folds. This fold shape—if correctly interpreted from the radar images without high resolution topographic data—is quite similar to fault-bend folds above a décollement, which are common on Earth[5]. The fact that the major fault-bend folds have nearly constant widths both along and across strike indicates a nearly constant depth to the décollement. In the area of eastern Artemis Chasma a regionally extensive décollement must extend for at least 50 km across strike and more than 350 km along strike.

The other important setting of foldbelts on Venus are the low-relief ridge belts found within the low plains of Venus. These were interpreted to be the result of compressional deformation based on Venera 15 and 16 radar images[6,7]. These belts are strongly concentrated in the region between 150° and 250° longitude and from 30° to 90° N, although they are present in other low plains of Venus. Magellan radar images show these ridge belts to be composed of anastomosing folds generally less than 10 km wide within foldbelts that can be over 100 km wide and thousands of kilometers long. Magellan altimetry show that the ridge belts have very little relief, rising at most 1 km higher than the surrounding plains (Figure 3b).

Near-surface deformation on Venus is interpreted to be brittle and is anticipated to be controlled by cohesive strength in the upper 1-2 km. The low-taper toes of foldbelts may be cohesion-dominated (Figures 2, 3a). Critical-taper wedge mechanics under anticipated Venus conditions[8] suggests that brittle wedges should have maximum surface slopes in the range 10-15°, which is similar to some estimated slopes in the steep parts of the foldbelts. Once the base of the wedge undergoes the brittle-plastic transition, the surface slope is expected to flatten to near horizontal in qualitative agreement with many topographic profiles of Venus (Figure 3b). The depth of the brittle-plastic transition is quite uncertain based on rock mechanics data, but is expected to be close enough to the surface to be strongly elevation-dependant because of atmospheric-temperature effects[8]. At higher elevations surface temperatures are lower;this increases the plastic strength of the wedge thereby increasing the depth to the brittle-plastic transition. The relief of foldbelts–measured between the toe of the wedge and the flat crest–displays a roughly linear dependence on absolute elevation (Figure 3c), ranging from 6 km for Maxwell Montes at an elevation of 10 km to a few hundred meters at the lowest planetary elevations (0 to –2 km). This remarkable phenomenon may be a result of increasing strength of mountain belts with decreasing surface temperature[9].

CHARACTERISTICS OF FOLD-AND-THRUST BELTS ON VENUS; Chris Connors and John Suppe

REFERENCES 1. Masursky, H. et. al., 1980, J. Geophys. Res., 85, 8232-8260. 2. Campbell, D. B. et. al., 1983, Science, 221, 644-647. 3. Basilevsky, A. T.et. al., 1986, J. Geophys. Res., 91, suppl., D378-D398. 4. Suppe, J and C. Connors, 1992, this volume. 5. Suppe, J., 1983, Amer. J. Sci., 283, 684-721. 6. Barsukov, V. L.et. al., 1986, J. Geophys. Res., 91, suppl., p. D378-D398. 7. Frank, S. H. and J. W. Head, 1990, Earth, Moon and Planets, 50/51, 421-470. 4. Dahlen, F. A. et. al., 1992, this volume. 9. Suppe, J and C. Connors, 1991, J. Geophys. Res. (submitted).

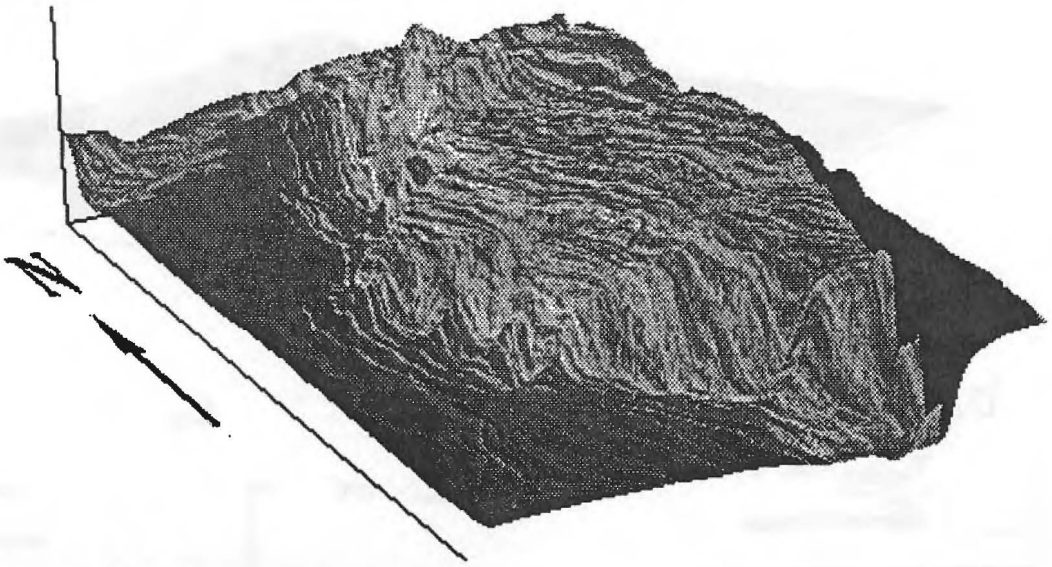

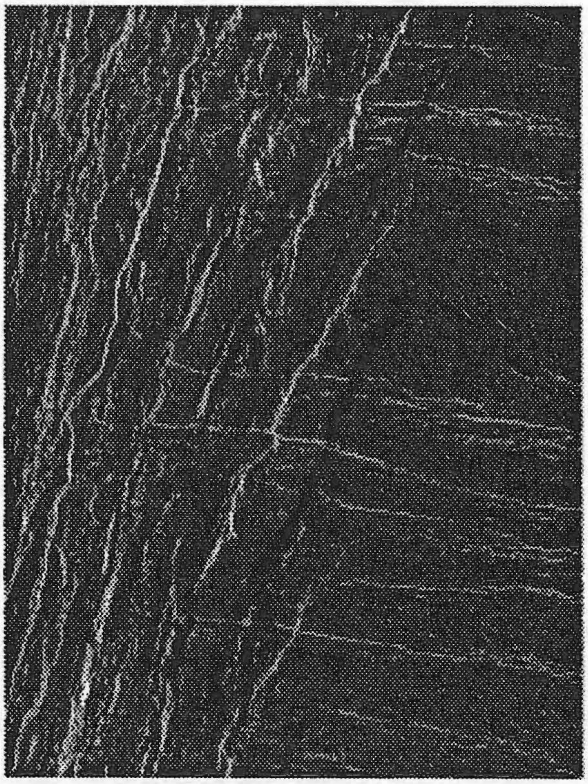

Figure 1. Oblique view of western Maxwell Montes. From west to east the foldbelt includes a flexural foredeep of undeformed high plains (radar dark) and deformed low taper toe (lines of bright radar return), an intensely deformed narrow zone of steep slopes (10-15°), and a relatively flat crest. The dark band on the eastern side is an area where there was a gap in SAR data but where altimetry was available. Vertical exageration = 5x.

Figure 2. SAR image of the toe of Artemis Chasma (132°, 35°S) with illumination from the left. Long northeast trending flat-topped anticlines are interpreted to be fault-bend folds stepping up from a regionally extensive decollement.

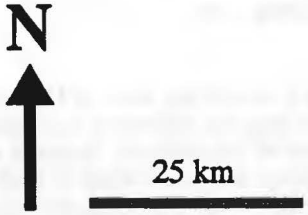

CHARACTERISTICS OF FOLD-AND-THRUST BELTS ON VENUS; Chris Connors and John Suppe

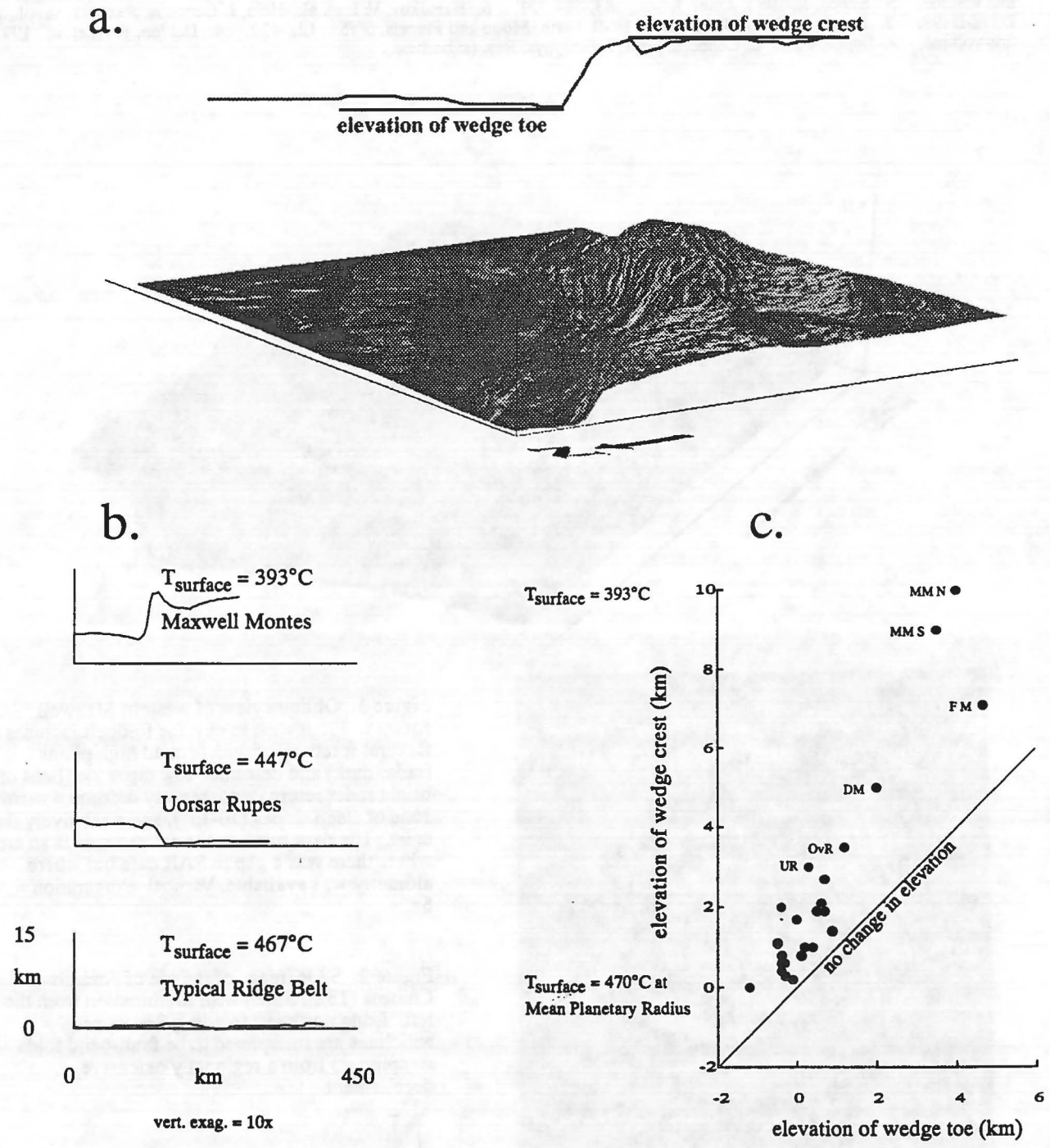

Figure 3. **a** is an oblique view of Uorsar Rupes (vertical exageration = 5x) showing the volcanically flooded foredeep, the deformed low taper toe, the narrow steeply sloped region, and the broad relatively flat crestal massif of this foldbelt. **b** shows examples of profiles of different foldbelts on Venus showing the dramatic change in overall relief of foldbelts as the elevation of the foldbelt crest (and surface temperature) changes. **c** shows this elevation dependence for foldbelts identified on Venus thus far. MMN-Maxwell Montes North, MMS-Maxwell Montes South, FM-Freyja Montes, DM-Danu Montes, OvR-Ovda Regio, UR-Uorsar Rupes.

CRITICAL-TAPER MODEL OF FOLD-AND-THRUST BELTS ON EARTH AND VENUS; F. A. Dahlen, John Suppe, Chris Connors and Evelyn Price, Department of Geological and Geophysical Sciences, Princeton University, Princeton, NJ 08544

The fold-and-thrust belts and submarine accretionary wedges that lie along compressive plate boundaries are one of the best understood deformational features of the Earth's upper crust. Although there is considerable natural variation among the many fold-and-thrust belts and accretionary wedges that have been recognized and explored, several features appear to be universal. In cross section, fold-and-thrust belts and accretionary wedges occupy a wedge-shaped deformed region overlying a basal detachment or décollement fault; the rocks or sediments beneath this fault show very little deformation. The décollement fault characteristically dips toward the interior of the mountain belt or, in the case of a submarine wedge, toward the island arc; the topography, in contrast, slopes toward the toe or deformation front of the wedge. Deformation within the wedge is generally dominated by imbricate thrust faults verging toward the toe and related fault-bend folding.

Mechanically, a fold-and-thrust belt or accretionary wedge on Earth or Venus is analogous to a wedge of sand in front of a moving bulldozer. The sand, rock, or sediment deforms until it develops a constant critical taper; if no fresh material is encountered at the toe, the wedge then slides stably without further deformation as it is pushed. The magnitude of the critical taper is governed by the relative magnitudes of the frictional resistance along the base and the compressive strength of the wedge material. An increase in the sliding resistance increases the critical taper, since it is the drag on the base that is fundamentally responsible for the deformation. An increase in the wedge strength, on the other hand, decreases the critical taper, since a stronger wedge can be thinner and still slide stably over a rough base without deforming. The state of stress within a critically tapered wedge is everywhere on the verge of failure, since the taper is attained by a process of continued deformation.

The critical taper of a wedge underlain by either a frictional or plastic décollement fault is given approximately by

$$\alpha + \beta \approx \frac{dH}{dx} \approx \frac{(1 - \rho_f / \bar{\rho}) + \mu_b(1-\lambda_b) + S_b/\rho g H}{(1 - \rho_f / \bar{\rho}) + 2(1-\lambda)(\sin \varphi)/(1 - \sin \varphi) + C/\rho g H}$$

Here α and β are the surface topographic slope and décollement dip, respectively; $\bar{\rho}$ and ρ_f are the mean density of a column of the wedge material and the pore fluid density, respectively; μ_b and λ_b are the coefficient of sliding friction and the Hubbert-Rubey pore-fluid pressure ratio on the décollement fault, respectively; φ and λ are the angle of internal friction and the pore-fluid pressure ratio just above the décollement fault; respectively; S_b and C are the plastic strength on the décollement fault and the uniaxial cohesive or plastic strength just above the décollement fault, respectively; H is the wedge thickness at horizontal position x, and g is the acceleration of gravity. The toe of a critically tapered fold-and-thrust belt or accretionary wedge may exhibit a narrower taper than the hinterland because of the dominance of cohesion. Once a wedge has grown large enough for its base to protrude beneath the brittle-plastic transition, the surface slope α should diminish to zero because of the abrupt reduction in shear traction on the décollement fault. This provides a natural

CRITICAL-TAPER MODEL OF FOLD-AND-THRUST BELTS ; Dahlen, Suppe, Connors and Price

explanation for the leveling off of mountain belts on both Earth and Venus, as illustrated below[1].

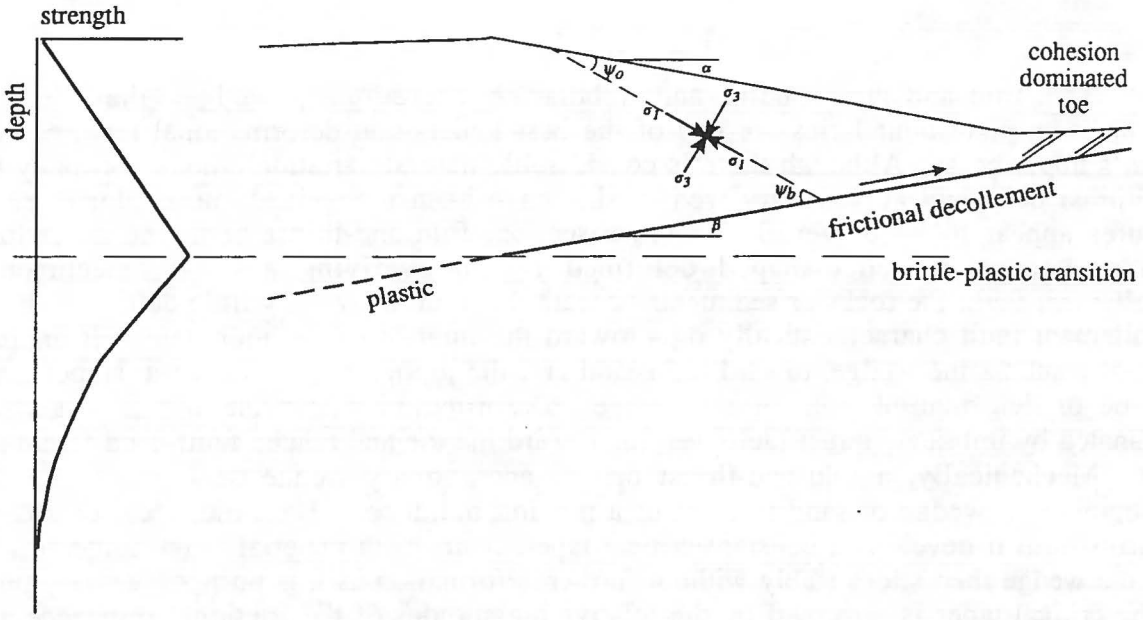

The most successful quantitative application of critical-taper theory on Earth is to the active fold-and-thrust belt in Taiwan. The regional structure and pore-fluid pressures in the Taiwan fold-and-thrust belt are well determined from data acquired during petroleum exploration, and this makes it an ideal natural laboratory for studying brittle frictional mountain building. the measured surface heat flow and known geometry of the Taiwan wedge are best fit by an effective coefficient of friction $\mu_b(1 - \lambda) = 0.16 \pm 0.06$. If the pore-fluid pressure ratio on the décollement is similar to that measured in several wells near the deformation front, then the coefficient of sliding friction on the Taiwan décollement fault is $\mu_b = 0.50 \pm 0.20$. This value is slightly lower than are laboratory friction measurements for most rocks (0.60 - 0.80), but it is within the range of measured friction values for clay-rich fault gouges (0.30 - 0.50).

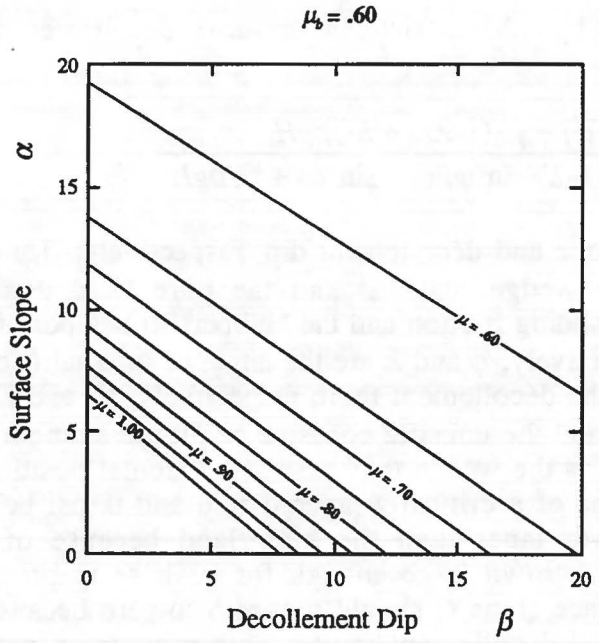

Critical-taper wedge theory, which has been quite successful for fold-and-thrust belts on Earth, may provide some indication

CRITICAL-TAPER MODEL OF FOLD-AND-THRUST BELTS ; Dahlen, Suppe, Connors and Price

of how they might form under the very different conditions of Venus. The low density atmosphere indicates that fluid pressures can be ignored, but the basaltic composition suggests the existence of a brittle cohesion-dominated boundary layer 1-2 km thick at the surface. The maximum surface slope of brittle wedges is predicted to be in the range 10°-15°, as shown at right; this is similar to current estimates of some of the steep-sloped regions of observed fold-and-thrust belts[1,2].

The low-taper toes of fold-and-thrust belts on Venus may be an effect of the cohesive boundary layer or alternatively of a low-strength plastic décollement. If the toe and steep-sloped regions are effects of brittle behavior then the flat tops may be a result of the brittle-plastic transition on the basal décollement. The depth to the brittle-plastic transition is quite uncertain from rock mechanics data, but is nevertheless predicted to be strongly elevation dependent because of the high atmospheric temperature (470° C at mean planetary radius) and the 100° C change in temperature over the range of planetary elevations, as shown below.

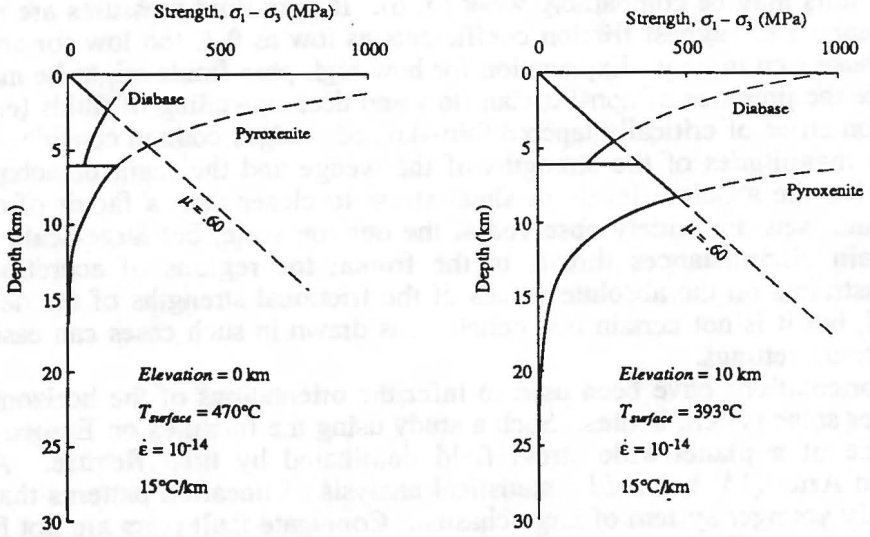

This predicted change in strength of the uppermost lithosphere with elevation may be the cause of the observed roughly linear relationship between the relief of foldbelts and their absolute elevations[1,2].

REFERENCES

1. Suppe, J and C. Connors, 1991, J. Geophys. Res. (submitted).
2. Connors, C. and J. Suppe, 1992, (this volume).

IMAGED FRACTURE SET ORIENTATIONS AND VENUS FAULT MECHANICS; Dan M. Davis and Adam E. Small, Department of Earth and Space Sciences, SUNY Stony Brook, Stony Brook, New York 11794.

A variety of recent studies suggest that some terrestrial faults may be much weaker than the surrounding rock. However, the mechanisms explaining this weakness are not well established. Because of the ways in which conditions differ from those on Earth, Venus may provide a useful laboratory for understanding the mechanics of frictional faulting in the lithospheres of terrestrial planets. Terrestrial geologists have long recognized the tendency of older faults on Earth to become reactivated even if they are not optimally oriented for the new stress regime. It is of interest to determine the geometric constraints controlling whether or not a fault set on Venus is reactivated, because those constraints contain information on the relative strengths of faulted and unfaulted rock.

Geothermal studies (1) indicate that the San Andreas fault lacks the pronounced geothermal anomaly that is to be expected if it slips at the high level of friction predicted by laboratory studies (2). This suggests that the shear traction along the San Andreas fault is low. Borehole data and regional fold axes near the San Andreas support this inference (3, 4). Other major strike-slip faults may be comparably weak (5, 6). If pore-fluid pressures are not extremely high, these data appear to suggest friction coefficients as low as 0.1, too low for any likely rock type, including those rich in clay. Explanation for how high pore-fluids might be maintained along the fault include the presence of non-Darcian flow and deep upwelling of fluids (e.g., 7, 8).

The geometries of critically tapered thin-skinned wedges contain considerable information on the relative magnitudes of the strengths of the wedge and the main detachment, but generally cannot resolve the absolute levels of shear stress to closer than a factor of about two (9), and conjugate fault sets are widely observed at the outcrop scale, but large-scale examples are rare. Under certain circumstances thrusts in the frontal toe regions of accretionary wedges may provide constraints on the absolute values of the frictional strengths of the deforming sediments (10, 11, 12), but it is not certain that conclusions drawn in such cases can easily be extrapolated to other tectonic settings.

Fault orientations have been used to infer the orientations of the horizontal principal stress axes on other solar system bodies. Such a study using the fractures on Europa (13) demonstrated the existence of a planet-wide stress field dominated by tidal flexure. A recent study of lineations on Ariel (14) has used a statistical analysis of lineation patterns that are distinct from the apparently younger system of large chasma. Conjugate fault pairs are not found, but in virtually every region with significant numbers of imaged fractures, the azimuthal distribution of features is bimodal, with two statistically significant peaks. Furthermore, these peaks tend to be arranged at virtually identical angles on either side of the horizontal principal stress axes predicted by a model tidal flexure model. The orientations of these peaks are consistent with friction, but with a coefficient of friction ($\mu \approx 0.2$) that is a factor of about three smaller than predicted by laboratory experiments (15).

Magellan images reveal many consistent fracture sets on the surface of Venus. We are at present carrying out a variety of statistical tests on features near Sedna Planitia to determine the consistency of the azimuths of the features within these sets, the radii of curvature of the rotations (if any) of the fracture sets, and the geometric relationships between crossing sets. In particular, we are interested in determining whether any crossing sets rotate in tandem as would be expected if they are contemporaneous and conjugate. In addition, we are interested in determining the range of observed angular relationships between crossing sets in order to constrain the degree to which pre-existing faults are weaker than unfaulted rock. The minimum angular deviation between a newly formed fault set and an older set that was not reactivated by the deformation that caused the second set is expected to depend very simply upon the difference between the strengths of faulted and unfaulted rock.

We find that in a local area, the fractures within a single fracture set are almost identical in azimuth; standard deviations of 1.5° to 3° within a set of dozens of fractures are common. These

sets commonly rotate along strike, with radii of curvature generally well in excess of 1000 km. Mutually crossing sets generally do not rotate together, suggesting that they are not contemporaneous and conjugate. This conclusion supports the inferences drawn in some cases based upon the geometric relationships between the sets, which suggest that one set preceeded the other. Thus far, the azimuthally closest crossing fracture sets that we have confirmed are about 20° apart.

In conclusion, an analysis of mutually crossing fracture sets on Venus offers the possibility of providing constraints on the relative weakness of Venusian faults compared with the unfractured country rock. Comparison with recent results on Earth may yield useful insights into the tectonics of Venus, the mechanics of faulting in rocky crusts, and the mechanisms responsible for the apparent weakness of at least some faults on Earth.

REFERENCES

1. Lachenbruch A.H. and Sass J.H. (1980) *J. Geophys. Res.*, **85**, 6185-6222.
2. Byerlee J. (1978) *Pure Appl. Geoph.*, **116**, 615-626.
3. Zoback M.D., Zoback M.L., Mount V.S., Suppe, J., Eaton J.P., Healy J.H., Oppenheimer D., Reasenberg P., Jones L., Raleigh C.B., Wong I.G., Scotti O. and Wentworth C. (1987), *Science*, **238**, 1105-1111.
4. Mount V.S. and Suppe J. (1987), *Geology*, **15**, 1143-1146.
5. Mount V.S. (1988), *Geol. Soc. Am. Abstr. with Progr.*, **20**, A320.
6. Mount V.S. (1989), Ph.D. Thesis, Princeton Univ., Princeton, NJ.
7. Byerlee J. (1990), *Geophys. Res. Lett.*, **17**, 2109-2112.
8. Rice J.R. (1991), in *Earthquake Mechanics, Rock Deformation, and Transport Properties of Rocks: a Symposium in honor of W.F. Brace.*
9. Davis D.M., Suppe J. and Dahlen F.A. (1983) *J. Geophys. Res.*, **88**, 1153-1172.
10. Dahlen F.A. (1984) *Annu. Rev. Earth Planet. Sci.*, **18**, 55-99.
11. Zhao W.-L, Davis D.M., Dahle F.A. and Suppe J. (1986), *J. Geophys. Res.*, **91**, 10246-10258.
12. Davis D.M. and von Huene, R. (1987), *Geology*, **15**, 517-522.
13. Helfenstein P. and Parmentier E.M. (1983) , *Icarus*, **53**, 415-430.
14. Nyffenegger P., Davis D.M. and Consolmagno G.J. (1991), *EOS Trans. AGU*, **72**, 184.
15. Beeman M., Durham W.B., Kirby S.H. (1988), *J. Geophys. Res.*, **93**, 7625-7633.

THE SOUTHERN AND CENTRAL APPALACHIANS AND THE GROWTH OF SE NORTH AMERICA, APPLICATIONS TO TECTONICALLY ACTIVE PLANETS

R. D. Hatcher, Jr., and P. J. Lemiszki, Dept. of Geological Sciences, University of Tennessee, Knoxville, TN 37996 and Environmental Sciences Division, Oak Ridge National Laboratory, Oak Ridge, TN 37831

The southern–central Appalachian orogen [SCA] is the product of closing of one or more oceans during Paleozoic compressional events following Late Proterozoic rifting and drifting, and a Paleozoic history that may record several partial to complete Wilson cycles. The history along the entire North American eastern margin was consistent until the Early Silurian, with formation of a Late Proterozoic rifted margin, an early Paleozoic passive margin, and destruction during the Penobscottian and Taconian (TAC, Ordovician) events with obduction of ophiolites, arc accretion, thrust and fold nappes, metamorphism, and plutonism. The Taconian event was diachronous — older (or a different event) in the south and New England, younger in the central Appalachians. Taconic allochthons occur only in the central Appalachians as the Hamburg klippe. Tectonic history of the internides is remarkably dissimilar along the length of the entire orogen throughout the remainder of the Paleozoic. Accretion of the Avalon/Carolina volcanic arc terrane probably occurred during the Taconian. Ordovician and Carboniferous–Permian plutons dominate in the southern and central Appalachians, but some Acadian (AC, Devonian) plutons also occur here. The extent of Acadian plutonism and metamorphism in the SCA is not clear, but may prove equally important. SCA tectonic style is dominated by TAC and Alleghanian (AL) cratonward–directed thrusts in both the internides and foreland, and dextral faults in the internides. Foreland clastic wedges indicate the extent of uplift during all three events: Taconian wedges are diachronous and extend along the SCA. A single AC wedge extends from New York to northern Virginia, and diachronous AL wedges extend from Pennsylvania to Alabama, and westward into the Ouachitas. AL collision with Africa may have been oblique — involving promontories along an irregular continental margin — producing mostly dextral AL faulting in New England, and the internal pull–apart Narragansett basin, but both overthrusts and dextral faulting in the SCA where collision may have been more head–on. Several buried terranes are present beneath the Coastal Plain in Florida, Alabama, and Georgia. AL foreland deformation overlaps Ouachita deformation beneath the Gulf Coastal Plain.

The Mesozoic history of this region involves the rifting of Pangaea and opening of the present Atlantic. This involved formation of a series of Late Tiassic–Jurassic rift basins along both margins, then opening of the ocean and formation of new ocean crust, cooling and contraction of the crust and downwarping of the continental margins to form the transgressive Upper Jurassic to Upper Cretaceous drift sequence. This was followed by regression beginning in the early Tertiary that may have marked a change from a pure extensional system into a new episode of compression related to ridge push, a stress system that continues until today.

Measurements of fractures from the Plateau, Valley and Ridge, Blue Ridge, and Piedmont of the southern Appalachians are being made to define global fracture

Southern and Central Appalachians. . .
Hatcher and Lemiszki

systems and to assess their tectonic significance related to both the Paleozoic and The Tertiary compressional and Mesozoic–Tertiary extensional history of southeastern North America. Because changes in the orientation of the regional stress field are related to plate–boundary forces, these changes should be reflected in the development of dominant fracture sets through time. In the southern Appalachians during different times in the Paleozoic, both the eastern and southern margins of North America were convergent plate boundaries; these same margins later evolved into divergent plate boundaries in the Mesozoic, and today are again under compression but also are part of plate interiors. The orientation of ths regional stress field during past tectonic activity can be predicted from other geologic criteria and compared with fracture orientations. Before evaluating their tectonic significance, however, it is important to separate out local fracture sets that have developed in response to changes in stress orientations associated with folding and faulting. Recognizing and differentiating local from regional fracture sets requires: (1) fracture analysis within different structural provinces; (2) fracture analysis across province boundaries; and (3) a comprehensive data set for regional extrapolation. Based on the data studied so far, we are able to present the following conclusions. Neotectonic joints form under the influence of the present–day stress field. Although few in number, available present–day stress measurements for the region suggest that such a joint set should be oriented approximately N50–60E and dip nearly vertically. A minor set is properly oriented in the Cumberland Plateau, but could be an older set, is poorly represented in the Valley and Ridge, but is evident in the Blue Ridge and Piedmont. Predictions of the orientation of the regional stress field during Mesozoic rifting are based on dike swarm orientations and structural analysis of rift basins. Although the regional stress orientation is assumed to have rotated during rifting, exsensive NW–striking dike swarms suggest that this particular stress orientation covered a regional extent in the southeastem U.S. Vertical NW–striking joints are evident throughout the region. Dating the joints in the Plateau is difficult because the regional stress field during the Paleozoic could have formed the NW set. Within the Valley and Ridge, however, a minor set oriented N35-55W and dipping near vertically is evident that cuts across bedding. Within the Piedmont and Blue Ridge, similar NW– striking vertical joint sets filled with low–T (zeolitic) minerals are also most likely of Mesozoic age considering that they accompany the dike swarms. Paleozoic fractures in the Piedmont form different sets with the oldest to youngest being filled with quartz–feldspar, quartz, quartz–epidote–calcite, and quartz–calcite–chlorite, respectively. The approximate orientation of the late Paleozoic orogenic stress field in the Plateau and Valley and Ridge can be inferred from regional fault and fold geometries. In the Valley and Ridge, a number of minor sets having a range of orientations formed in relation to faulting and folding and are not of a regional extent. Major joint sets striking N50-60E and N30-40W, and perpendicular to bedding, occur in the Plateau and restored beds of the Valley and Ridge, suggesting that they predate thrusting. It is uncertain, however, whether these sets formed in relation to

Southern and Central Appalachians. . .
Hatcher and Lemiszki

basin–forming stresses or plate–boundary covergent tectonics. Resolution of much of this chronology can be made using remote–sensing techniques, but on–ground sampling of fractures for determination of compositions of fillings will be needed to refine some of the relationships between fracture systems and relative chronology of development.

MAXWELL AND THE ANDES: SIMILIARITIES AND CONTRASTS, W.M. Kaula, A. Lenardic, D. L. Bindschadler, University of California, Los Angeles.

Maxwell Montes, the highest structure of Venus (the peak is 11 km above mean planetary radius [MPR]) is clearly the most likely site on the planet for contemporary tectonics. It has a steep western front, with a slope similar to the suboceanic part of the Andes (figure 1). The entire slope of this front is marked by an intense series of parallel folds and thrust faults at 15-25 km spacing, interpreted as due to failure under compression of a shallow crustal zone of weakness (Zuber, 1987).

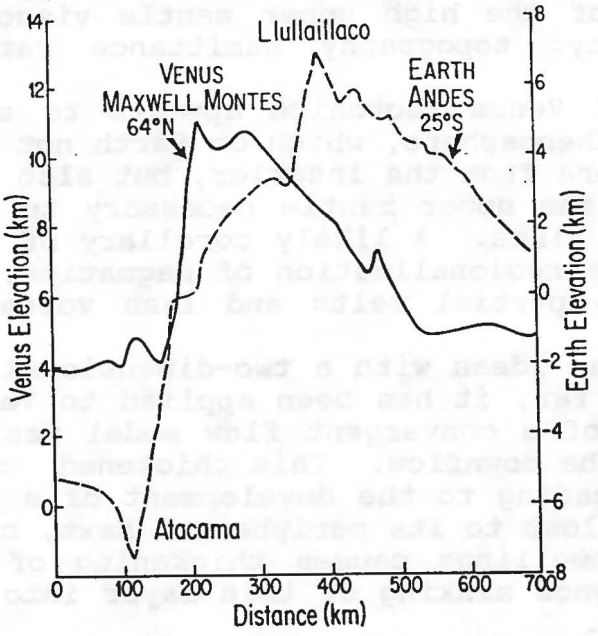

Fig. 1: Cross-sections

Evidences of gravitational modification are confined to the flanks of Maxwell Montes, 600 km north and 300 km south of the peak. Volcanism appears only on the east slope, about 200 km from the crest, and seems to be entirely triggered by the great impact crater Cleopatra. These lava flows are quite massive, and suggest that Maxwell is a great accumulation of relatively weak material, that must still be in the building phase.

500 km beyond the crest the terrain levels off, although still at an appreciable height, 4 km, above MPR. This terrain, western Fortuna Tessera, extends almost 1000 km further eastward before further significant drop. It is characterized by a series of sub-parallel arcuate ridges, also at spacings of 15-25 km. (Kaula et al, 1992).

The two cross sections in Figure 1 are similar, although the Andes have a much more marked trench and are about 40 percent wider. The Andes are also much longer than Maxwell Montes. Along this stretch, there is appreciable variation in cross section; in particular, to north of the figure the Altiplano broadens to about 400 km. Another difference is that the volcanism is confined to the western Cordillera, and does not occur on the eastern slope. (Isacks, 1988; Kono et al, 1989).

Despite these differences, it is tempting to draw comparisons between the two structures, with Fortuna Tessera and the Brazilian Shield both being older, more stable terrains whose resistances contribute significantly to the pile-up of the mountains. However, the source of the thrusting from the west is much more evident for the Andes: an oceanic lithosphere moving more than 10 cm/yr (with respect to the hot-spot frame) from a rise 4000 km away. In the case of Maxwell, a line normal to its ridge lines hits within 500 km of the front a steep 2 km scarp at the southern edge of Lakshmi Planum, and beyond that further

irregular terrain without any broadscale orientation analogous to the spreading Pacific floor. To the north of such a line there is the more homogeneous province of Lakshmi Planum, but its main slope is from north to south, and its northern part contains appreciable ancient-looking ridged terrain.

The driver for Maxwell must be deeper, more mantle- and less lithosphere-associated than that for the Andes. This obscurity is typical of mountain regions on Venus. In particular, Ishtar's structure evidences that the pattern of flow can vary appreciably over a few hundred kilometers within Venus: a contrast to the Earth's oceans, where patterns are controlled over 1000's of kilometers by the tectonic plates. This spatial variability occurs in spite of the high upper mantle viscosity required by the high gravity: topography admittance ratios. (Solomon et al, 1992).

This regional character of Venus tectonics appears to arise from the lack of a shallow asthenosphere, which on Earth not only acts to decouple the lithosphere from the interior, but also enables the lateral mobility of the upper mantle necessary to provide a voluminous flow to the rises. A likely corollary of this small scale of mantle flows is regionalization of magmatism, resulting in smaller percentage partial melts and less volcanism and plutonism. (Kaula, 1992).

We are testing some of these ideas with a two-dimensional finite element computation. So far, it has been applied to Venus-like conditions. The result of a convergent flow model was the thickening of the crust over the downflow. This thickened crust resisted further squeezing, leading to the development of a plateau and the shifting of downflows to its periphery. Next, crustal shortenings over the downwellings causes thickening of the mantle boundary layer, and thence sinking of this layer into the mantle. (Lenardic et al, 1992).

Throughout the progress of the Ishtar model, strong coupling is maintained between the surface layers and the interior. Adoption of Earth-like conditions, with a less viscous asthenospheric layer, is expected to lead to enhancement of downwelling compared to the last phase of the Venus model described above, because there is both a stronger push from the spreading oceanic lithosphere and less resistance to downwelling in the upper mantle.

The foregoing primary circumstances still leave in doubt the secondary consequences that are the main subject of difference between the hypotheses of Isacks (1988) and Kono et al (1989): the uplift of the Altiplano Puna. This problem has its analogue in the uplift of Maxwell Montes, which Vorder Brugge and Head (1990) suggested arose from both imbrication near the surface and plastic deformation at depth. This hypothesis is more similar to that of Isacks (1988)-- lithospheric thinning and crustal shortening-- than that of Kono et al (1989)-- massive magmatism. But the Earth's asthenosphere may have its back-arc effects as well, leading to a much readier transfer of matter by secondary convection, induced by the subduction. To answer these questions may require the incorporation of some approximation to magmatic differentiation, which has not yet been attempted.

References

Isacks, B. L. 1988: Uplift of the central Andean plateau and bending of the Bolivian Orocline. *J. Geophys. Res.* 93, 3211-3231.

Kaula, W. M. 1992: Compositional evolution of Venus. *Chemical Evolution of the Earth and Planets*, E. Takahashi, ed., Springer-Verlag, submitted.

Kaula, W. M. & 5 others 1992: Styles of deformation in Ishtar Terra and their implications. *J. Geophys. Res.* 97, submitted.

Kono, M., Fukao, Y. & Yamamoto, A. 1989: Mountain building in the central Andes. *J. Geophys. Res.* 94, 3891-3905.

Lenardic, A., Kaula, W. M. & Bindschadler, D. L. 1992: The tectonic evolution of western Ishtar Terra, Venus. *Geophys. Res. Let.* 19, accepted.

Solomon, S. C. & 7 others 1992: Venus tectonics: an overview. *J. Geophys. Res.* 97, submitted.

Vorder Bruegge, R. W. & Head, J. W. 1990: Tectonic evolution of eastern Ishtar Terra, Venus. *Earth, Moon, & Planets* 50/51, 251-304.

Zuber, M. T. 1987: Constraints on the lithospheric structure of Venus from mechanical models and tectonic surface features. *J. Geophys. Res.* 92, E541-551.

RHEOLOGY OF THE CRUST AND UPPER MANTLE OF VENUS: CONSTRAINTS IMPOSED BY LABORATORY EXPERIMENTS; D.L. Kohlstedt, Department of Geology and Geophysics, Pillsbury Hall, University of Minnesota, Minneapolis, MN 55455

Analysis of the tectonic processes on Venus that have produced its anomalously high surface relief requires accurate, experimentally derived flow laws for the predominant crustal and mantle rocks. To date, mantle deformation has been modeled based on laboratory derived rheologies for olivine and pyroxene [e.g., (1,2)], reflecting an upper mantle with a peridotitic or eclogitic composition. Crustal deformation has been modeled using the measured rheology for diabase [e.g., (3,4)], because the Venusian crust appears to have a basaltic composition.

While the rheologies of olivine-rich rocks [e.g., (5,6)] and, to a lesser extent, pyroxene-rich rocks [e.g., (7,8)] have been reasonably well determined, the mechanical properties of rocks of basaltic composition have been the subject of relatively few laboratory studies. Although experimentally obtained flow laws for Maryland diabase have been reported [e.g., (9,10)], the presence of hydrous phases in this rock results in a substantial amount of partial melting at temperatures as low as 900°C; in this rock, partial melting is accompanied by an extensive amount of fracturing. In addition, breakdown of the hydrous phases may lead to water-weakening of some of the crystalline phases.

This paper will present a critical review of the published experimental rheologies for rocks of compositions similar to those believed to comprise the crust and upper mantle of Venus. In the case of olivine-rich rocks, for example, the primary focus will be on the effect of water on high-temperature creep strength [e.g., (5,11)]. In contrast, for rocks of basaltic compositions, the emphasis will be on the rheologies of the constituent phases [e.g., (8,12)], in order to avoid the complications associated with the presence of hydrous phases. Thus, approaches for calculating the flow laws of polyphase aggregates from the flow laws of the appropriate end-member minerals will be discussed [e.g., (13,14)]. The results of such calculations will be compared to strengths measured for both as-received and pre-dried diabase rocks.

Acknowledgement: The author is indebted to Steve Mackwell for his help in the preparation of this abstract.

1. Turcotte D.L. (1989) *J. Geophys. Res. 94*, pp. 2779-2785.
2. Phillips R.J. (1990) *J. Geophys. Res. 95*, pp. 1301-1316.
3. Zuber M.T. (1987) *J. Geophys. Res. 92*, pp. E541-E551.
4. Grimm R.E. and Solomon S.C. (1988) *J. Geophys. Res. 93*, pp. 11,911-11,929.
5. Karato S., Paterson M.S. and Fitz Gerald J.D. (1986) *J. Geophys. Res. 91*, pp. 8151-8176.
6. Bai Q., Mackwell S.J. and Kohlstedt D.L. (1991) *J. Geophys. Res. 96*, pp. 2441-2463.
7. Ave'Lallemant H.G. (1978) *Tectonophys. 48*, pp. 1-27.
8. Raterron P. and Jaoul 0. (1991) *J. Geophys. Res. 96*, pp. 14,277-14,286.
9. Kronenberg A.K. and Shelton G.L. (1980) *J. Struct. Geol. 2*, pp. 341-353.
10. Caristan Y. (1982) *J. Geophys. Res. 87*, pp. 6781-6790.
11. Mackwell S.J., Kohlstedt D.L. and Paterson M.S. (1985) *J. Geophys. Res. 90*, pp. 11,319-11,333.
12. Tullis J. and Yund R.A. (1991) *J. Struct. Geol. 13*, pp. 987-1000.
13. Chen I.W. and Argon A.S. (1979) *Acta Metall. 27*, pp. 785-791.
14. Tullis T.E., Horowitz F.G. and Tullis J. (1991) *J. Geophys. Res. 96*, pp. 8081-8096.

THE THERMAL STRUCTURE OF MOUNTAIN BELTS ON VENUS: VOLCANISM AND MANTLE HEAT FLOW IN THE FREYJA MONTES REGION;

Noriyuki Namiki and Sean C. Solomon, Department of Earth, Atmospheric, and Planetary Sciences, Massachusetts Institute of Technology, Cambridge, MA 02139

Introduction. The linear mountain belts of Ishtar Terra on Venus are notable for their topographic relief and slope and for the intensity of surface deformation [1,2]. The mountains surround the highland plain Lakshmi Planum, the site of two major paterae and numerous other volcanic features and deposits [3,4], and evidence is widespread for volcanism within the mountains and in terrain immediately outward of the mountain belt units [2,4]. While the mountains are generally regarded as products of large-scale compression of the crust and lithosphere [2,5], whether western Ishtar Terra is a site of mantle upwelling and consequent hot spot volcanism [6-8] or of mantle downwelling and consequent convergence of lithospheric blocks [9,10] is currently a matter of debate. If the upwelling model holds, then volcanism in Lakshmi Planum and presumably within the mountains and adjacent terrain is likely a result of pressure-release partial melting in the upwelling mantle [6-8]. If the downwelling model is appropriate for western Ishtar Terra, then partial melting in the underlying mantle is less likely and the volcanism may require remelting of thickened crust [9,10]. While these two hypotheses for magmatism can be distinguished on the basis of the chemistry of the melts [11], chemical data are presently lacking for the Ishtar region.

The competing hypotheses for magmatism in western Ishtar Terra can also be tested with thermal models, given a kinematic or dynamic model for the evolution of the region. In this paper we assess the crustal remelting hypothesis by means of kinematic and thermal models for the Freyja Montes deformation zone [12]. Specifically, we consider the conditions under which these thermal models are consistent with the observational constraints on magmatism in the region.

Observational Constraints on Magmatism. Volcanism in the Freyja Montes deformation zone is spatially heterogeneous. Both plateaus to the north and south of the mountain belt, Lakshmi Planum and Itzpapalotl Tessera, show evidence for widespread volcanic deposits and landforms. The foredeep at the base of Uorsar Rupes is embayed by comparatively undeformed volcanic flows of the North Polar Plains. In the Freyja Montes belt, however, Magellan images show little evidence for volcanism [4].

Under the crustal remelting hypothesis, while volcanism is widespread in Lakshmi Planum and in Itzpapalotl Tessera, the absence of volcanism in Freyja Montes requires explanation since the topographically higher Freyja Montes should, on isostatic grounds, have a thicker crust than plateaus and therefore a greater volume of hot lower crust susceptible to remelting. Possible explanations are; (1) volcanism occurs in Freyja Montes but horizontal strain is sufficiently rapid that volcanic features are rendered unrecognizable in radar images, (2) magma is generated beneath Freyja Montes but erupts at lower elevations on the plateaus, (3) magma is generated beneath Freyja Montes but is denser than the solid crust and does not ascend, or (4) magma is not generated beneath Freyja Montes because of a lower thermal gradient in the crust of the mountain belt than in that of the plateau.

On the basis of petrogenetic considerations it has been argued that, under anhydrous conditions, shallow crustal remelting (< 50 km) produces highly fluid ferrobasaltic magmas while deeper crustal remelting (> 50 km) results in more SiO_2-rich melt products such as trondhjemites, andesites, and basaltic andesites [11]. As noted below, simple Airy isostatic models suggest that the thickness of the crust is less than 50 km beneath the plateaus but greater than 50 km beneath the mountain belt. The volcanic deposits on the outboard plateau, Itzpapalotl Tessera, appear to have formed by the eruption of highly fluid lavas, consistent with a ferrobasaltic composition [4]. Thus the lavas that most recently erupted onto the outboard plateau are consistent with their generation by remelting of the underlying crust; and magmas generated by remelting of the lower crust beneath the mountains will be, if anything, less dense than those generated by crustal remelting beneath the plateaus. These inferences render unlikely the second and third explanations above. The first and last possibilities are testable by calculating the thermal structures consistent with kinematic models of crustal deformation.

THERMAL STRUCTURE OF MOUNTAIN BELTS: Namiki N. and Solomon S.C.

Thermal Models. We first calculate the critical heat flow for crustal remelting beneath plains, plateaus, and mountain belts. Then we estimate the heat flow from the mantle from two-dimensional advective thermal models of crustal strain and associated mantle flow.

To calculate the critical mantle heat flow for crustal remelting we use the simple one-dimensional steady-state conductive heat equation. We assume that the physical properties of crustal material are those of anhydrous basalt. The pressure-dependent solidus is taken from [13]. The critical heat flow from the mantle is the minimum value necessary to remelt crust; this critical heat flow depends on the thickness of the crust and the crustal heat source abundance. The abundances measured by Venera and Vega landers range from 2.5×10^{-11} to 2.0×10^{-10} W/kg [14]. Critical heat flow is plotted as a function of crustal thickness and heat generation in Figure 1. At a given crustal thickness, heat flow from the mantle needs to be higher than the critical value in order for remelting to occur. For a 20-km-thick crust beneath the plains and simple Airy compensation of topographic relief, typical crustal thicknesses of the plateau and the mountain belt are 37 and 61 km, and their critical heat flow values are 32 and 15 mW/m^2, respectively. Of course, for time-dependent thermal models, these values are only approximate guides, and the actual temperature structure must serve as the basis for a melting criterion.

Heat flow from the mantle depends on the flow field associated with crustal deformation. Here we solve the problem of mantle flow given the kinematics of crustal deformation. We assume uniform horizontal strain rates e_{xx} within the outboard plateau and in the mountain belt. Horizontal and vertical velocities, u and w, at the base of crust are determined by integrating the strain rate in both directions. These velocities serve as boundary condition at the top of mantle. We solve the equations of motion for irrotational, incompressible flow in the mantle The boundary condition along the north side (North Polar Plains) is $w = 0$ and along the south side (Lakshmi Planum) is $u = 0$. Velocities are required to be finite as $z \rightarrow \infty$. The normalized mantle temperature T is determined from the given flow field and the advective heat equation under the boundary conditions $T = 0$ and $T = 1$ at the top and bottom, respectively, and $\partial T/\partial x = 0$ along the north and south sides. The mantle flow field for an illustrative model (e_{xx} beneath the mountain belt and outboard plateau is 2×10^{-15} and 10^{-15} s^{-1}, respectively) is shown in Figure 2, and the associated temperature field is shown in Figure 3.

The resulting heat flow from the mantle is shown in Figure 4. Heat flow is normalized by the value of heat flow in the plains. Heat flow from the mantle is 0.5-0.9 beneath the outboard plateau and 0.1-0.2 beneath the mountain belt. On the basis of estimates of the average global heat flow in the range 50-74 mW/m^2 [15-17], we take the heat flow in the plains to be 60 mW/m^2. The corresponding heat flow is 36-54 mW/m^2 beneath the plateau and 6-12 mW/m^2 beneath the mountain belt. Therefore mantle heat flow exceeds the critical value beneath the plateau, so crustal remelting is expected, while heat flow is less than critical value beneath the mountain belts, and volcanism by crustal remelting is not expected.

Also shown in Figure 4 are results for a model with strain rates an order of magnitude less that for the model in Figures 2 and 3. These models indicate that a strain rate less than 10^{-16} s^{-1} is required if crustal remelting is to be expected beneath the mountain belts. On the basis of this result, the suggestion above that volcanism may be occurring in Freyja Montes but be rendered unrecognizable by ongoing strain must be considered unlikely.

Conclusions. Volcanism in Itzpapalotl Tessera can be explained by crustal remelting if heat flow from the mantle is more than 32 mW/m^2 in that region, while the absence of volcanism and crustal remelting in Freyja Montes requires the mantle heat flow there to be less than 15 mW/m^2. These conditions are satisfied by a spatially heterogeneous heat flow from the mantle associated with a downwelling flow field consistent with surficial tectonics.

References. [1] V.L. Barsukov et al., *JGR, 91*, D378, 1986; [2] S.C. Solomon et al., *Science, 252*, 297, 1991; [3] K.M. Roberts and J.W. Head, *EMP, 50/51*, 193, 1990; [4] J.W. Head et al., *Science, 252*, 276, 1991; [5] L.S. Crumpler et al., *Geology, 14*, 1031, 1986; [6] A.A. Pronin, *Geotectonics, 20*, 271, 1986; [7] A.T. Basilevsky, *Geotectonics, 20*, 282, 1986; [8] R.E. Grimm and R.J. Phillips, *JGR, 96*, 8305, 1991; [9] K.M. Roberts and J.W. Head, *GRL, 17*, 1341, 1990; [10] D.L. Bindschadler and E.M. Parmentier, *JGR, 95*, 21329, 1990; [11] P.C. Hess and

THERMAL STRUCTURE OF MOUNTAIN BELTS: Namiki N. and Solomon S.C.

J.W. Head, *EMP, 50/51*, 47, 1990; [12] J.W. Head, *Geology, 18*, 99, 1990; [13] H.S. Yoder and C.E. Tilley, *J. Petrol., 3*, 342, 1963; [14] Y.A. Surkov et al., *Proc. Lunar Planet. Sci. 17th, JGR, 92*, E537, 1987; [15] R.J. Phillips and M.C. Malin, *Ann. Rev. Earth Planet., Sci., 12*, 411, 1984; [16] S.C. Solomon and J.W. Head, *JGR, 87*, 9236, 1982; [17] M.T. Zuber, *Proc. Lunar Planet. Sci. 17th, JGR, 92*, E541, 1987.

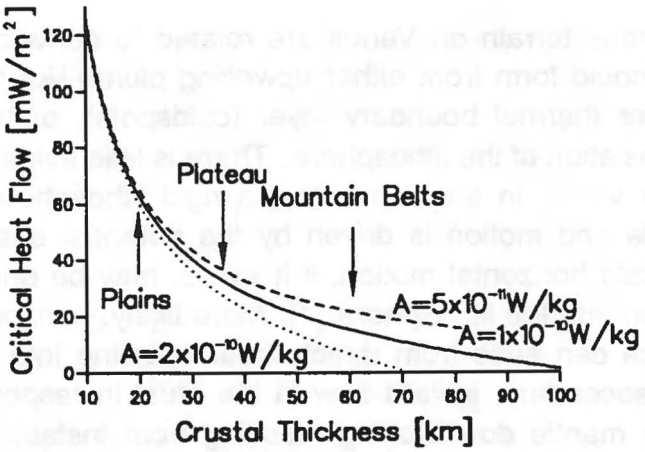

Figure 1 Critical heat flow for crustal remelting as a function of crustal thicknesses and crustal heat production A. Crustal thicknesses in the plateau and the mountain belt estimated under Airy isostasy and a 20-km-thick crust beneath the plains are shown by arrows.

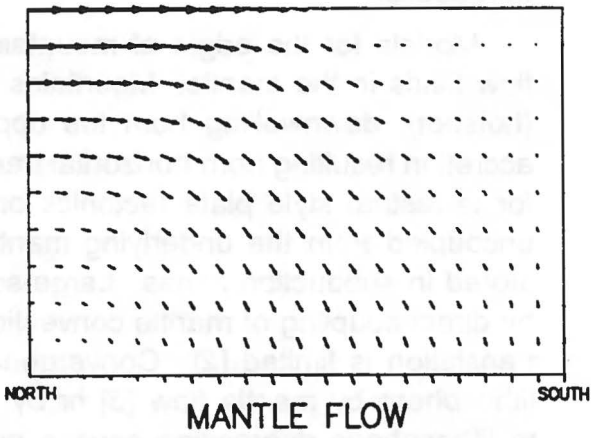

Figure 2 Model of downwelling mantle flow; see text.

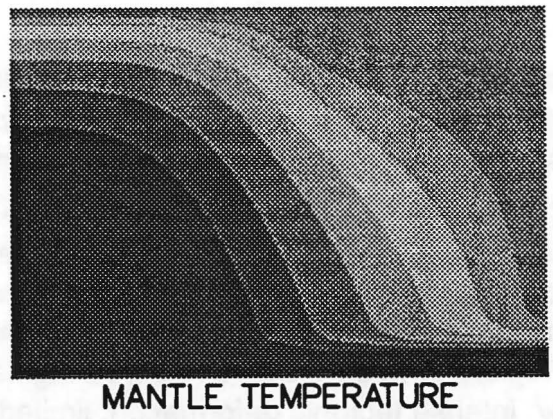

Figure 3 Temperature field determined for the flow model in Figure 2.

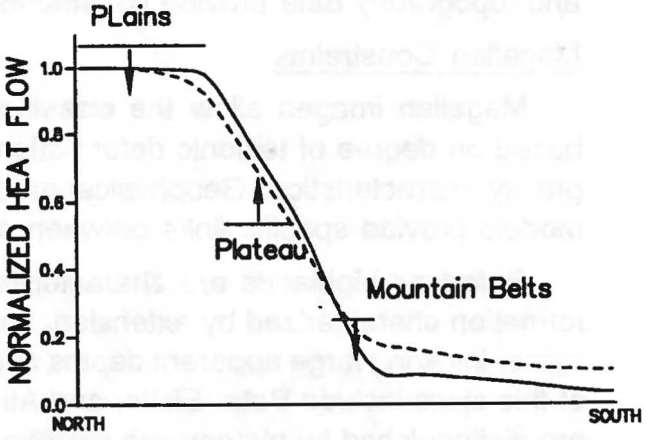

Figure 4 Heat flow at the top of mantle. The solid line corresponds to strain rates of 10^{-15} s^{-1} in the plateau and $2x10^{-15}$ s^{-1} in the mountain belt, and the dashed line corresponds to strain rates of 10^{-16} s^{-1} in the plateau and $2x10^{-16}$ s^{-1} in the mountain belt. Critical heat flows for plains, plateau, and mountain belt are shown as horizontal lines.

GEOPHYSICAL CONSTRAINTS ON VENUSIAN MOUNTAIN BELTS

R.J. Phillips[1] and R.E. Grimm[2] 1. Dept. of Geological Sciences, SMU, Dallas, TX 75275 & Dept. of Earth and Planetary Sciences, Washington Univ., St. Louis, MO 63130. 2. Dept. of Geology, Arizona State Univ., Tempe, AZ 85287.

Introduction

Models for the origin of mountainous terrain on Venus are related to convective flow fields in the mantle. Mountains could form from either upwelling plume-like flow (hotspot), downwelling from the upper thermal boundary layer (coldspots), or from accretion resulting from horizontal translation of the lithosphere. There is little evidence for terrestrial style plate tectonics on Venus in the sense that a rigid lithosphere is uncoupled from the underlying mantle and motion is driven by the potential energy stored in subduction zones. Large-scale horizontal motion, if it exists, may be driven by direct coupling of mantle convection into the lithosphere [*1*]. More likely, horizontal translation is limited [*2*]. Convergence can arise from direct shear coupling into the lithosphere by mantle flow [*3*] or by secondary, inward flow in the crust in response to lithospheric depression caused by mantle downwelling resulting from instabilities developed in the upper thermal boundary layer of convection [*4*]. Convergence can also be obtained by mantle plume impingement on the base of the lithosphere, provided there are lateral heterogeneities in the strength of the lithosphere [*5*]. Thus vertical convective motion may lead to significant amounts of horizontal lithospheric strain. Convergence by either of these mechanisms could lead to folded mountain belts and to lithospheric thrust faulting and subduction-like morphology. Long wavelength gravity and topography data provide constraints on all of these models.

Magellan Constraints

Magellan images allow the classification of highlands into three distinct classes based on degree of tectonic deformation, style of tectonism, regional morphology and gravity characteristics. Geophysical models can be tested against each class; further, models provide specific links between classes.

Beta-type highlands are characterized by broad topographic rises, moderate deformation characterized by extension, shield volcanism, and large geoid to topography ratios, implying large apparent depths of compensation (ADC) of topography. Members of this class include Beta, Eistla, and Atla Regiones. In contrast, *Ovda-type* highlands are distinguished by plateau-like morphology, intense tectonic deformation, limited volcanism, and moderate ADCs. Ovda and Thetis Regiones belong to this group. Ishtar Terra is a unique region on Venus, so that a single feature belongs to the *Lakshmi-type* classification. Lakshmi Planum is plateau-like, with narrow mountain belts on its periphery, moderate volcanism, and a large ADC.

Tessera terrain, such as Alpha and Tellus Regiones, most nearly resemble Ovda-type highlands in gross geological characteristics; however their ADC values appear to be 30 km or less. They are linked in evolutionary sequences to geophysical models, as discussed below.

GEOPHYSICAL CONSTRAINTS: Phillips, R.J. and Grimm, R.E.

Model Evolution and ADC Variability

Both upwelling and downwelling models lead to specific sequences of variability in geology, morphology, and ADC. In either case, transitional forms of evolution should be observed on Venus.

Hotspot Models. The evolution of an upwelling mantle plume and the attendant hotspot has been discussed in some detail in *Phillips et al.* [*2*]. A hotspot evolutionary sequence is characterized by: (i) a broad domal uplift resulting from a rising mantle plume, (ii) massive partial melting in the plume head and generation of a thickened crust or crustal plateau, (iii) collapse of dynamic topography as the plume wanes, and (iv) creep spreading of the crustal plateau. The ADC during this sequence gradually shallows as the plume wanes and as the crustal thickness increases due to magmatic activity.

Several sources of stress are present in the lithosphere during the plume cycle. These include (i) largely extensional deformation associated with uplift [*3*], (ii) forces associated with ductile detachments, which may lead to thickened crust residing on the slopes of uplifts [*6*], (iii) membrane compressional forces acting on the new crustal block as dynamic topography subsides, (iv) extensional and compressional forces associated with collapse and spreading of the crustal block, and (v) thermoelastic stresses as the hotspot cools, particularly in the new crustal cap. The superposition of several sources of stress will lead to complex deformation of a crustal plateau.

A proposed observational sequence of the hotspot cycle is Beta Regio → Thetis Regio → Ovda Regio → Alpha Regio. Lakshmi Planum is treated as a special case wherein a plume has impinged on a pre-existing tessera, and the lateral variation in lithospheric strength, from tessera to non-tessera, is able to focus flow stresses, giving rise to peripheral mountain belts.

Coldspot Models. The evolution of a cold, downwelling plume and the attendant coldspot evolution has been discussed by *Bindschadler and Parmentier* [*4*] and *Bindschadler et al.* [*7*]. A coldspot evolutionary sequence is characterized by: (i) downward surface displacement in response to the sinking plume, (ii) crustal flow inward, leading to crustal thickening and formation of a crustal plateau on a time-scale of several hundred million to a billion years, (iii) rebound of the crustal plateau to increased elevation as the cold plume is assimilated by the mantle, and (iv) collapse and creep spreading of the crustal plateau. The ADC during the coldspot cycle is increasingly positive and reaches a discontinuity (ADC = ∞) when the topography passes through zero in its second-stage evolution; thereafter it is negative and asymptotically increases to a small positive value.

The tectonic cycle during coldspot evolution is one of compressional strain focusing near the margins of the growing plateau; later the crustal plateau is in extension as it spreads laterally. A proposed observational sequence of the coldspot cycle is Atalanta Planitia → Ovda Regio → Alpha Regio → Lakshmi Planum.

GEOPHYSICAL CONSTRAINTS: Phillips, R.J. and Grimm, R.E.

We note that if crustal flow is indeed an important process on Venus, then hotspots evolve into basins more readily than coldspots into crustal plateaus. Furthermore, in either case, after the topography passes through zero, the topography and free-air gravity will be anti-correlated for a long geological period. This is not observed on Venus.

Model Testing with Magellan Data

At this stage, tests of these models with Magellan data have been very limited. There is no question, for example, that Ovda and Thetis Regiones have undergone intense tectonic deformation. However, there is not agreement as to the sign of the accumulated strain, or, for that matter, whether or not the geophysical models are sufficiently sophisticated to take advantage of detailed geological information. It is difficult to place the role of tessera terrain such as Alpha Regio into either the upwelling or the downwelling model. The most reasonable interpretation of these regions is that they are long-lived crustal blocks that have been subject to repeated episodes of tectonic deformation, oftentimes exogenic in origin and related to very large scale stress patterns.

Regions that satisfy pre-Magellan notions of hotspots are simpler tectonically and have fared somewhat better; specific stress predictions from dynamic models for Eistla Regio match well the major tectonic fabrics in the central part of this region [*8*].

Refinement of geophysical models can be expected when Magellan enters the gravity acquisition phase of its mission. The spacecraft will gather, during its fourth cycle around the planet, gravity field information superior to existing data in both resolution and signal-to-noise ratio. Subsequent circularization of the orbit will enable characterization of lateral variations in density beneath Ishtar Terra. Such issues as the degree of compensation of the mountain belts and the presence or absence of descending slabs on the margins of Ishtar can be addressed.

References

1. J.W. Head and L.S. Crumpler, *Nature* **346**, 525 (1990).
2. R.J. Phillips, R.E. Grimm, and M.C. Malin, *Science* **252**, 651 (1991).
3. R.J. Phillips, *J. Geophys. Res.* **95**, 1301 (1990).
4. D.L. Bindschadler and E.M. Parmentier, *J. Geophys. Res.* **95**, 21,239 (1990).
5. R.E. Grimm and R.J. Phillips, *Geophys. Res. Lett.* **17**, 1349 (1990).
6. S. Smrekar and R.J. Phillips, *Geophys. Res. Lett.* **15**, 693 (1988).
7. D.L. Bindschadler, G. Schubert, and W.M. Kaula, *Geophys. Res. Lett.* **17**, 1345 (1990).
8. R.E. Grimm and R.J. Phillips, submitted to *J. Geophys. Res.*, 1991.

INVESTIGATIONS OF THE SURFACE OF VENUS USING MAGELLAN DATA.
R. Stephen Saunders, Jet Propulsion Laboratory, California Institute of Technology, Pasadena, CA 91109

The Magellan radar data set comprises radar images, radiometry, and data derived from the altimetry. These data are obtained by the 12.6 cm wavelength radar system. The image mode is a synthetic aperture system that obtains 120 to 300 meter radar resolution. For comparison with conventional photography, this resolution corresponds approximately to 240-600 m line-pair resolution. The images are processed to 75 m pixels. Topographic resolution of the altimetry is about 50 m. The altimeter footprint is 10 to 30 km, increasing from periapsis altitude of 300 km to the polar altitude of 2200 km. a global topographic map with 5 km pixels has been constructed. In the passive radiometry mode, the receiver can distinguish relative microwave brightness temperatures of about 2 K. Global emissivity maps with 5 km pixels have been constructed from the radiometry mode. Other global data sets are the rms-slope and Fresnel reflectivity.

The Magellan spacecraft is in a 3.26 hour, near polar orbit. The full-resolution basic image data record (FBIDR) consists of one orbit of data. As an image, one orbit is a strip 20 km wide and about 15,000 km long. Image mosaics have been made from the SAR data. A subset of the globe has been made into full-resolution, 75 m pixel, (F-MIDR) mosaics. Compressed resolution global coverage mosaics include 3x3 averaged mosaics with pixel dimensions of 225 m, 675 m, and 2025 m. All these mosaic products are 8192 by 7168 pixels. Coverage through cycle 2, 16 months of mapping, is about 92% with left-looking nominal incidence angle profile and about 40% right looking at constant 25 deg incidence angle.

Interpretation of the image data requires understanding of the effects of the incidence angle, which varies with latitude in the nominal mapping profile. Some understanding of the way the radar signal is scattered by the surface is also necessary. The reflected or backscattered signal is controlled by local slope, roughness and intrinsic reflectivity. Use of multiple coverage obtained by the left- and right-looking modes is helpful. Synthetic stereo images have been constructed using the altimetry and image mosaics. These are helpful for visualizing regional slopes and terrain shapes.

COUPLING BETWEEN MANTLE CONVECTION AND CRUSTAL DEFORMATION ON VENUS;

Mark Simons, Sean C. Solomon, and Bradford H. Hager, Department of Earth, Atmospheric, and Planetary Sciences, Massachusetts Institute of Technology, Cambridge, MA 02139.

Introduction. High-resolution Magellan images and altimetry of Venus reveal a wide range of styles and scales of surface deformation [1]. This deformation cannot readily be described within the classical terrestrial plate tectonic paradigm. A key difference between Earth and Venus may be the degree of coupling between the motions of the convecting mantle and the overlying lithosphere. The high correlation of long-wavelength topography and gravity and the large apparent depths of compensation suggest that Venus lacks an upper-mantle low-viscosity zone [2-5]. If so, then mantle convection should indeed couple strongly to the lithosphere, and patterns of mantle flow should have recognizable signatures in surface topography and deformation [6,7].

Models. We explore the effects of this coupling using finite element modelling techniques. The crust and mantle in these models are treated as viscous fluids, and we solve both the equations of motion and the heat equation at every time step. A modified version of the 2-D Cartesian finite-element program ConMan [8] is employed. A passive marker chain tracks the crust-mantle interface and permits variation in the crustal buoyancy as well as specific crustal and mantle rheologies. These rheologies depend on composition, temperature and stress. In addition to the flow field, the stress field in the lithosphere and the surface topography are readily calculated. An example of these models is presented here. We use an irregular finite-element mesh that is 28 elements high and 80 elements wide. Our maximum resolution is in the 40-km-thick top layer, where each element is 4 km high and 10 km wide. In all, the mesh is 800 km in the horizontal dimension and 400 km in the vertical dimension. We impose free-slip boundary conditions on the

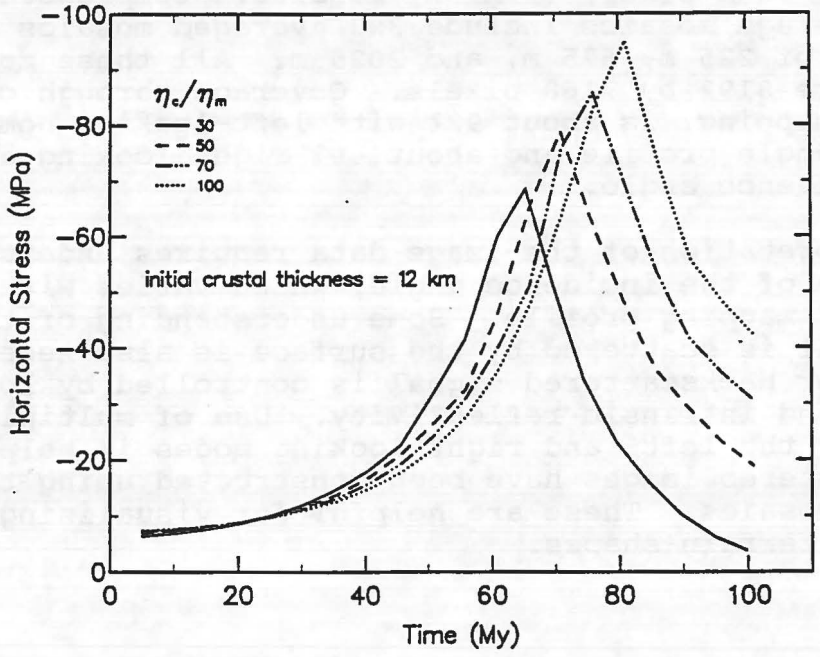

Figure 1. Development of horizontal stress vs. time. The stress is measured at the top of the model box over the downwelling. The peak stress corresponds to the point when the surface elevation reaches a minimum.

CRUSTAL DEFORMATION ON VENUS: Simons M. et al.

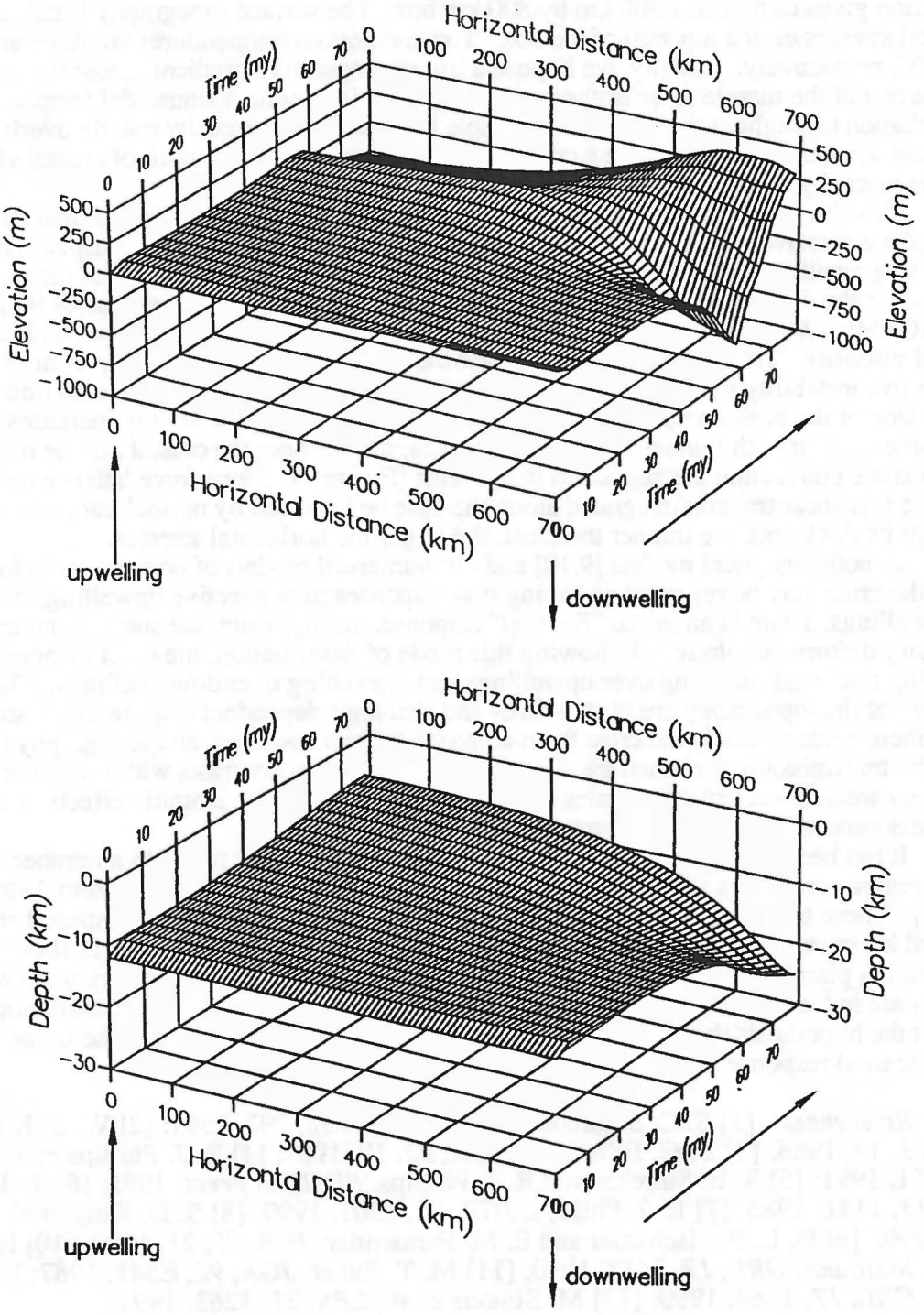

Figure 2. Top: Evolution of the surface topography with time. Bottom: Evolution of the crust-mantle interface with time. Both figures are for a model with an initial crustal thickness of 12 km and a ratio of crustal viscosity to mantle viscosity of 70.

CRUSTAL DEFORMATION ON VENUS: Simons M. et al.

top and side walls, with no flow through these walls. We apply a no-slip condition on the bottom boundary, while vertical flow through this boundary is unconstrained. In effect, this last boundary condition gives us a virtual 800 km by 800 km box. The surface topography is calculated from the vertical stresses on the top wall of the box. Top and bottom temperatures are fixed at 500°C and 1250°C, respectively. Initially, we impose a linear temperature gradient across the lithosphere and set the rest of the mantle to be isothermal. Flow is initiated with a sinusoidal temperature perturbation throughout the box. Our example has a constant-viscosity mantle overlain by a constant-viscosity crust. We use a crustal thickness of 12 km and a ratio of crustal viscosity to mantle viscosity of 70.

Results. In all our models, convection produces horizontal compressional stresses in lithosphere that overlies downwelling mantle and extensional stresses in lithosphere that overlies upwelling mantle. As the convective vigor increases so does the magnitude of the compressive stress over the downwelling, with stress in the crust reaching values in excess of 90 MPa in less than 100 My. We find that the rate of increase in compressive stress decreases with increasing crustal viscosity. This is because the stronger the crust, the more the development of the convective instability in the mantle driving the deformation is impeded. We also find that the magnitude of the peak compressive stress achieved above the downwelling increases with higher viscosities and/or with thinner initial crustal layers; the stronger the crustal lid, the more tractions from mantle convection are supported in the crust (Figure 1). Since force balance on the crust requries that shear traction integrated along the base be balanced by normal tractions integrated through its thickness, the thinner the crust, the larger the horizontal stresses.

In both analytical models [9,10] and our numerical models of convection-induced crustal flow, the crust may be regarded as having two responses to convective upwellings and downwellings. There is an initial "flexural" response, during which the surface and crust-mantle boundary deform "in phase." Following this mode of deformation, the crust responds by changing thickness, thinning over upwellings and thickening over downwellings. The amplitude and sign of the topography are highly time- and rheology-dependent (Figure 2). A strong mantle lithosphere tends to shield the crust from convective shear tractions, and topography results mainly from the transmission of normal tractions induced by density contrasts within the mantle. A relatively weak lower crust facilitates crustal deformation, and the isostatic effects of crustal thickness variations dominate the topography.

It has been suggested that the distinct linear zones or belts found in a number of lowland plains regions on Venus result from lithospheric instabilities induced by horizontal stresses [11,12]. These belts are 50-200 km wide, several hundred kilometers long, spaced several hundred kilometers apart, and are generally elevated by several hundred meters above the surrounding plains. As the models in this paper demonstrate, significant horizontal compressive stresses are induced in crust that overlies a convective downwelling. These calculations thus support the hypothesis that ridge belts occur as a result of this stress during the transition from the initial flexural response to the later phase of crustal thickening [13].

References: [1] S. C. Solomon et al., *Science, 252*, 297, 1991; [2] W. S. Kiefer et al., *GRL, 13*, 14, 1986; [3] B. G. Bills et al., *JGR, 92*, 10, 1987; [4] R. J. Phillips et al., *Science, 252*, 651, 1991; [5] S. E. Smrekar and R. J. Phillips, *EPSL, in press*, 1991; [6] R. J. Phillips, *GRL, 13*, 1141, 1986; [7] R. J. Phillips, *JGR, 95*, 1301, 1990; [8] S. D. King et al., *PEPI, 59*, 195, 1990; [9] D. L. Bindschadler and E. M. Parmentier, *JGR, 95*, 21, 1990; [10] H. Schmeling and G. Marquart, *GRL, 17*, 2417, 1990; [11] M. T. Zuber, *JGR, 92*, E541, 1987; [12] M. T. Zuber, *GRL, 17*, 1369, 1990; [13] M. Simons et al., *LPS, 21*, 1263, 1991.

GRAVITATIONAL SPREADING OF PLATEAUS AND MOUNTAIN BELTS ON VENUS

Suzanne E. Smrekar, and Sean C. Solomon, Department of Earth, Atmospheric, and Planetary Sciences, Massachusetts Institute of Technology, Cambridge, MA 02144.

Introduction. On Earth, the extreme elevation of such areas as the Himalayas and the Andes creates sufficient potential energy to drive lateral extension, even within an overall convergent regime. Gravitational spreading is likely to be even more important on Venus than on Earth because erosion does not rapidly destroy the topography and the higher surface temperature weakens the crust [1,2]. The highest relief on Venus is found in Ishtar Terra. Within Ishtar Terra, the plateau of Lakshmi Planum rises 3-4 km above mean planetary radius and is surrounded by the mountain belts of Danu, Akna, Freyja, and Maxwell Montes, which rise another 1.5, 3, 3, and 7 km above the plateau, respectively. The distribution of impact craters in the northern 25% of Venus, including Ishtar Terra, indicates a crater retention age of 50 My-1 Ga [3,4]. Although the distribution of impact craters cannot be used to date regions as small as a mountain belt or even all of Ishtar Terra, such an average age raises the question of how such high topography can be maintained for periods comparable to the crater retention age, given the expected weakening effect of the surface temperature (~740 K) on the rheology [1]. In this study we address this question. Recently acquired Magellan radar images (120-210 m resolution) make it possible to observe evidence for gravitational spreading in the form of small-scale extension [5,6]. Altimetry data (9-25 km footprint) allow correlation of slope with extension. Below we discuss the evidence for gravitational spreading in Ishtar Terra and finite element models of this process designed to investigate the implications of the observations for tectonic evolution of the region.

Observations. We recognize gravitational spreading by analogy with features observed on Earth. Extensional faulting is expected to develop parallel to the margin of a plateau, or perpendicular to topographic slope. In the case of active convergence, extension occurs typically parallel to the direction of shortening [7]. If the relief is great enough, extension can also occur perpendicular to the direction of shortening [8]. In the radar images, graben appear as long, narrow troughs. Numerous examples of extensional faulting are visible in Ishtar Terra. In Akna Montes, extensional faulting is observed parallel to the apparent direction of shortening. Extensional faults are locally the latest stage of deformation and are oriented perpendicular to topographic slope in Freyja Montes. In Danu Montes, one large graben (10 km wide, 50 km long) is cut by later compressional features. On the northern and southern margins of Maxwell Montes, two graben sets occur, one parallel and one perpendicular to topographic slope. Extensional faulting is prevalent along the margin of Lakshmi Planum and is generally parallel to the plateau margin. Estimated strain in these areas is approximately 5-15% but may be much larger if blocks are rotated along the normal faults. This observational evidence for gravitational spreading is discussed more fully in [6].

Models. We use the finite element algorithm TECTON [9] to model the evolution of gravitational spreading in a vertical section of the crust near the margin of a plateau or the edge of a broad mountain range. The model employs a depth-dependent, viscoelastic rheology with non-linear stress dependence and exponential temperature dependence. We adopt a diabase flow law [10], consistent with measurements of the composition of surface material sampled in the equatorial plains [11], a Young's modulus of 6×10^{10} Pa, and a Poisson's ratio of 0.25. Temperature at the surface is taken to be 740 K and to increase linearly with depth. Each row of elements in the grid (Figure 1) has the same viscosity, which is equivalent to assuming that the temperature is constant along the bottom and top of the grid. This results in a lower thermal gradient beneath the plateau than beneath the plains. The boundary conditions are zero vertical velocity on the bottom of the grid, a free surface top boundary, and zero horizontal velocity at the sides. The bottom boundary condition approximates an upper mantle layer that is much stronger than the lower crust. Brittle failure in the models is evaluated using a Mohr-Coulomb criterion. Details of the models are given in [6].

The timing of predicted brittle failure and relaxation of the relief are found for ranges of plateau height, plateau margin slope, crustal thickness, and thermal gradient. Slopes of 1-30° and plateau

GRAVITATIONAL SPREADING ON VENUS: Smrekar S.E. and Solomon S.C.

or mountain belt heights of 1-6 km are observed in Ishtar Terra. Crustal thickness on Venus is expected to be 10-30 km, based on models of viscous relaxation of impact craters [12] and of the formation of periodic tectonic features [13]. Scaling the heat flux from Earth to Venus by planetary mass gives an estimate of average thermal gradient of 10-25 K/km [14,15].

Two time steps in the deformation history of an illustrative model are shown in Figure 1. This model has initially a 6-km-high plateau or mountain range, a bounding scarp of slope 30° (such as are observed on the western slope of Maxwell Montes), and a 30-km-thick crust and a thermal gradient of 15 K/km in the plains. The first predicted failure (normal faulting) in this model occurs on the plateau, at only 10^{-4} y after spreading begins. Normal faulting near the base of the scarp occurs by 10^{-2} y (Figure 1a). As relaxation of the topography begins, the failure becomes more localized near the surface, and the base of the scarp is pushed up, causing further normal faulting (Figure 1b). At 10^{3} y, shallow thrust faulting in the plains is predicted at distances greater than 40 km from the base of the scarp. Relaxation of the topography occurs primarily through flow in the lower crust.

Failure and relaxation of topography occur more rapidly for thicker crust, and in the case of failure, for greater plateau heights. Thus the model illustrated in Figure 1 is among the most rapidly deforming cases. For the parameter range studied, failure is predicted in the plateau within 10^{5} y, even for a plateau height of 1 km and a crustal thickness of 10 km. In most cases, failure on the slope occurs shortly after failure on the plateau; thrust faulting in the plains occurs typically only for a crustal thickness of 30 km. When failure is first predicted, the horizontal surface strain is typically 0.05%. This strain is unlikely to be recognized as normal faulting in Magellan radar images; a strain of 1% is probably a more reasonable value to compare with observations. Strains of this magnitude do not accumulate at the surface until 10^{4}-10^{7} y. As these models do not explicitly include faulting, there is some uncertainty in the interpretation of the calculated strain after the initial failure. Once faulting is initiated, stress might be more easily accommodated by movement along the fault plane than by additional failure. Thus strain may be underestimated in these models.

Significant relaxation of relief also occurs rapidly on geologic time scales. As topographic slopes in the mountain belts and on the plateau margins and the average elevation in Ishtar Terra are among the highest on the planet, we assume that relief has not relaxed by more than 25% of its original value. For a thermal gradient of 15 K/km, 25% relaxation occurs within 10^{4}-10^{7} y for all of the cases considered (Figure 2). Relaxation of the topography is accomplished primarily through flow in the lower crust and thus depends strongly on the effective viscosity at the base of the crust. The viscosity is controlled by temperature (in this study, by the combination of crustal thickness and thermal gradient), and to a lesser degree by the deviatoric stress. Plateau height and scarp slope thus have little effect on the relaxation rate.

Discussion. Both failure and relaxation of the relief occur on geologically rapid time scales for observed values of topographic elevation and slope, and for typical values of thermal gradient and crustal thickness. This result may be interpreted as indicating that the topography in Ishtar Terra is either stronger than indicated by laboratory flow laws, or has been maintained by tectonic forces until times significantly less than 10^{7} y. The primary evidence in favor of an anomalously strong crust is the large crater retention age (50 My-1 Ga) of the northern portion of Venus. However, this value has a large uncertainty, and the age of smaller regions may deviate significantly from the average age. The widespread presence of volcanism in Ishtar Terra, which in many locations appears to have been contemporaneous with extension, argues against a strong, cold crust. The large apparent depth of compensation at Ishtar Terra (180 km) indicates that the long-wavelength topography (> 2000 km) is dynamically compensated [16]. This dynamic compensation suggests a source of stress to actively maintain the short-wavelength topography. For these reasons, we favor the hypothesis that topography-building processes in Ishtar Terra have been active until times at least as recent as 10^{6}-10^{7} y ago.

References. [1] J. Weertman, *Phys. Earth Planet. Inter., 19*, 197-207, 1979; [2] S. Smrekar and R.J. Phillips, *Geophys. Res. Lett., 15*, 693-696, 1988; [3] B.A. Ivanov, et al., *J. Geophys. Res., 91*, D413-430, 1986; [4] G.G. Schaber, et al., *Solar System Res., 21*, 89-93, 1987; [5]

GRAVITATIONAL SPREADING ON VENUS: Smrekar S.E. and Solomon S.C.

S.C. Solomon, et al., *Science, 252*, 297-312, 1991; [6] S.E. Smrekar and S.C. Solomon, *J. Geophys. Res.*, submitted, 1991; [7] R. Armijo, et al., *J. Geophys. Res., 91*, 13,803-13,872, 1986; [8] B.C. Burchfiel and L.H. Royden, *Geology, 13*, 679-682, 1985; [9] H.J. Melosh and A. Rafesky, *Geophys. J. R. Astron. Soc., 60,* 333-354, 1980; [10] Y. Caristan, *J. Geophys. Res., 87*, 6781-6790, 1982; [11] Yu.A. Surkov, et al., *J. Geophys. Res., 92*, E537-540, 1987; [12] R.E. Grimm and S.C. Solomon, *J. Geophys. Res., 93*, 11,911-111,929, 1988; [13] M. T. Zuber and E. M. Parmentier, *Icarus, 85*, 290-308, 1990; [14] W.M. Kaula and J.R. Phillips, *Geophys. Res. Lett., 8*, 1187-1190, 1981; [15] S.C. Solomon and J.W. Head, *J. Geophys. Res., 87*, 9236-9246, 1982; [16] R.E. Grimm and R.J. Phillips, *J. Geophys. Res., 96*, 8305-8324, 1991.

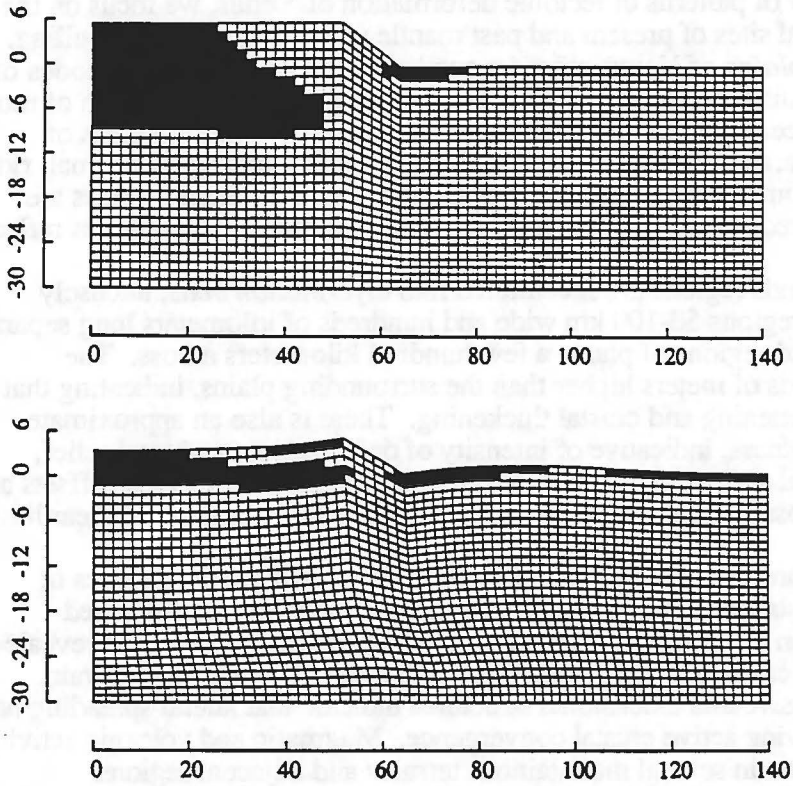

Figure 1. (Top) Finite element grid at approximately 0.1 y after spreading begins. Units are in km. Elements that are predicted to fail by normal faulting are shaded. The elements are 2 km wide and 1 km high. The vertical exaggeration is 1.5:1. (Bottom) Grid at approximately 10^3 y. Thrust faulting is predicted in the plains farther than 40 km from the scarp. The plateau elevation has decreased by approximately 25%.

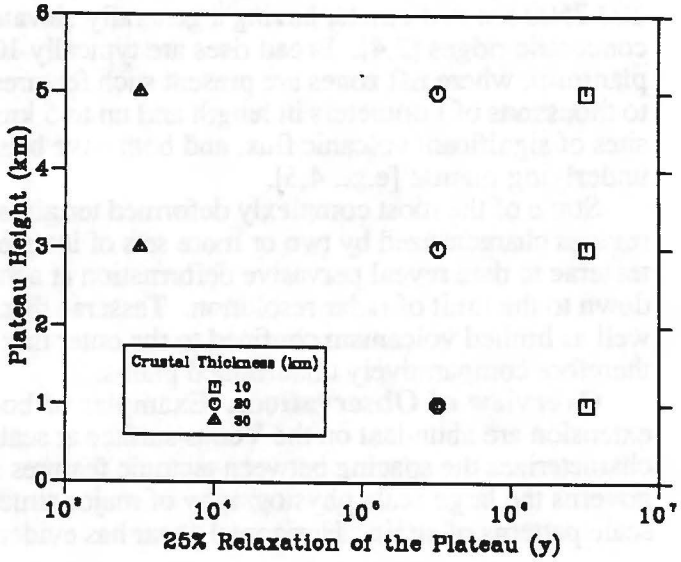

Figure 2. The time at which the height of the plateau has relaxed by 25% is shown as a function of plateau height for three values of plains crustal thickness. The thermal gradient in the plains is taken to be 15 K/km, and the initial slope of the bounding scarp is 3°. Effective viscosities at the base of a crust 10-30

VENUS: AN OVERVIEW OF GLOBAL AND REGIONAL TECTONICS;

S.C. Solomon, Dept. of Earth, Atmospheric, and Planetary Sciences, M.I.T., Cambridge, MA 02139.

Introduction. Radar imaging and altimetry data from the Magellan mission have revealed a diversity of deformational features at a variety of spatial scales on the Venus surface [1]. The radar images from Magellan constitute an improvement in resolution by at least an order of magnitude over the best images previously available [e.g., 2,3]. In this paper we discuss what those images, and their interpretations, are revealing about the styles of lithospheric deformation on Venus, the mechanical properties of the lithosphere, and their implications for the tectonic history of the planet. Following an overview of patterns of tectonic deformation of Venus, we focus on the question of identifying potential sites of present and past mantle upwelling and downwelling.

Tectonic Features. The *plains* of Venus record a superposition of different episodes of deformation and volcanism. This deformation is manifested in areally distributed strain of modest magnitude and in zones of concentrated lithospheric extension and shortening. In areas of distributed deformation, the characteristic spacing between tectonic features (graben, small ridges, or narrow lineations) ranges from 1 km or less to tens of kilometers. The strain patterns are commonly coherent over hundreds of kilometers, implying that even many local features reflect a long-wavelength processes.

Much of the strain in lowlands regions is concentrated into *deformation belts*, intensely deformed linear to curvilinear regions 50-100 km wide and hundreds of kilometers long separated by radar-dark and less deformed regions of plains a few hundred kilometers across. The deformation belts stand hundreds of meters higher than the surrounding plains, indicating that they are products of lithospheric shortening and crustal thickening. There is also an approximate correlation between radar brightness, indicative of intensity of deformation, and total relief, presumably a measure of crustal shortening. A number of older linear features show offsets and changes in trend where they cross deformation belts, indicating that some horizontal shear has accompanied shortening.

Mountain belts, which are present only in Ishtar Terra, represent still greater degrees of lithospheric shortening and crustal thickening. Modest horizontal shear has accompanied compression in several mountain belt regions. Magellan images have for the first time revealed widespread evidence for lateral extension and gravitational collapse of mountainous terrain. Relationships between compressive and extensional structures indicate that lateral spreading has occurred both during and following active crustal convergence. Magmatic and volcanic activity has accompanied the lateral extension in several mountainous terrains and adjacent regions.

Venus displays two principal geometrical variations on large-scale lithospheric extension: the quasi-circular *coronae* and *broad rises* with linear rift zones. Coronae are circular to oval structures 200-2500 km in diameter having a generally elevated interior and a narrow deformed annulus of concentric ridges [2,4]. Broad rises are typically 1000-3000 km in diameter and quasi-circular in planform; where rift zones are present such features are 50 to several hundred kilometers wide, up to thousands of kilometers in length and up to 5 km in relief. Both coronae and rifted rises are sites of significant volcanic flux, and both have been attributed to convective upwelling in the underlying mantle [e.g., 4,5].

Some of the most complexly deformed terrain are the *tesserae*: broad, elevated, radar-bright regions characterized by two or more sets of intersecting linear features [2]. Magellan images of tesserae to date reveal pervasive deformation at a variety of scales, ranging from tens of kilometers down to the limit of radar resolution. Tesserae display significant (5 km or more) local relief as well as limited volcanism confined to the outer margins and isolated interior pockets of smooth and therefore comparatively undeformed plains.

Overview of Observations. Examples of both horizontal shortening and horizontal extension are abundant on the Venus surface at scales ranging from the 1-km scale that characterizes the spacing between tectonic features in a number of regions to the 1000-km scale that governs the large scale physiography of major structures and the spatial coherence of many smaller scale patterns of strain. Horizontal shear has evidently occurred in the lowland deformation belts

and in the mountain belts, but such shearing tends to be broadly distributed and to accompany horizontal stretching or shortening. No clear examples have yet been documented of long, large-offset strike-slip faults such as those typical of oceanic and some continental areas on Earth.

The various scales of deformation arise from the complicated mechanical and dynamical structure of the Venus interior. The 10-30 km scale is plausibly attributed to the response of a strong upper crustal layer, while the deformation of a strong upper mantle layer can account for tectonic features with characteristic scales of a few hundred kilometers [6]. The scale of a few hundred to a few thousand kilometers, particularly if evident in the long-wavelength gravity as well as the topography, is likely dominated by mantle convection and its associated dynamic stresses and heat transport. The scale of a few kilometers and less involves either internal deformation of the upper crust or tectonic disruption of a thin surficial layer decoupled thermally or mechanically from the remainder of the otherwise strong upper crust.

In the absence of significant weathering and erosion, the lifetime of high topography is limited by ductile flow in the thickened lower crust that must at least partly support the topographic relief once active compression ceases. The widespread evidence for lateral extension in the mountains of Ishtar Terra documents the tendency for such ductile flow to occur. The very steep regional slopes (20-30°) marking some of the edges of Lakshmi Planum and the front ranges of the mountain belts provide evidence that dynamical processes have been recently operative.

There is little or no evidence for tectonic behavior similar to terrestrial oceanic regions, i.e., nearly rigid lithospheric plates with horizontal dimensions of 10^3-10^4 km and active deformation confined to plate boundary zones a few kilometers to tens of kilometers across. Analogues to oceanic fracture zones and to deep sea trenches have been suggested [7], but they are not common. Much of the tectonic behavior on Venus appears to be most reminiscent of actively deforming continental regions on Earth, with deformation distributed across broad zones one to a few hundred kilometers wide separated by comparatively stronger and less deformed blocks having dimensions of hundreds of kilometers. On Earth, the continental lithosphere in tectonically active areas is weaker than typical oceanic lithosphere because of the greater thickness of more easily deformable crust. Because of the much greater surface temperature on Venus, the lithosphere on Venus should behave in a weak manner for crustal thicknesses less than are typical of continental regions on Earth.

In general, the intensity of deformation and state of preservation of tectonic features on Venus are strong functions of local topographic relief. Elevated regions tend to be areas of thicker crust and therefore a thicker layer of weak lower crust susceptible to ductile flow. Such regions thereby serve as concentrators of regional lithospheric strain, such as the lowland deformation belts and the mountainous terrain. Elevated regions, particularly areas uplifted by compression and crustal shortening, are also less susceptible to volcanic resurfacing and thus are more likely to preserve records of deformation spanning one or more episodes of significant strain. Much of the surface of Venus may have only two possible fates: volcanic burial and comparatively long-term preservation as relatively elevated and intensely deformed terrain. The first fate is represented by the abundant volcanic plains. The second fate may be primarily represented by tessera terrain.

Patterns of Mantle Convection A major challenge in unravelling the evolution of Venus is to understand the interaction between mantle convection and the lithosphere. The strong correlation between long-wavelength gravity and topography and the large (100-400 km) apparent depths of compensation of relief for many upland regions [8] suggests that these long-wavelength variations are signatures of mantle dynamics [9,10]. These apparent depths of compensation and considerations of probable lithosphere thickness on Venus point to the absence of a low-viscosity zone beneath the lithosphere [11,12], in contrast to the situation in oceanic regions on Earth [13]. The lack of a low-viscosity zone, possibly a result of the dehydration of the upper mantle of Venus [14], allows mantle dynamic stresses to couple strongly to the overlying lithosphere and can thus contribute significantly to surface topography and tectonic deformation [12,15].

These considerations raise the question as to whether the geometry of upper mantle convection on Venus may be discerned directly from measurements of topography and gravity and observations of lithospheric deformation and igneous activity. In numerical models of three-

dimensional convection in constant-viscosity spherical shells with Rayleigh numbers at about 100 times the critical value, convective upwelling occurs dominantly in the form of cylindrical plumes, with the number and characteristic spacing of plumes a function of the relative fraction of basal and internal heating [16]. With parameters appropriate to the Venus mantle and with 20% of the heating supplied from below, a figure consistent with the heat flux from the core given by parameterized convection models of Venus thermal evolution [17], such calculations indicate that about 20 plumes are active at any one time [18], although this result is likely to be quite sensitive to such model assumptions as choice of Rayleigh number and viscosity structure.

Localized centers of mantle upwelling are likely to be characterized by broad topographic rises and geoid highs [19], by uplift and extension of the lithosphere, and by consequent pressure-release melting and surface volcanism [20]. Long-wavelength topography and geoid anomalies on Venus are characterized by a number of broad highs such as might be produced by 10-20 distinct centers of approximately cylindrical upwelling [10,11], although specification of the geoid is presently limited by the uneven resolution of gravity information with latitude and the necessary truncation of harmonic representations. A number of these highs correspond to the broad rises, 1000-3000 km across, identified from radar imaging as centers of volcanism and tectonic activity [1,3,21], also consistent with sites of active mantle upwelling. A complementary question is the location of sites of mantle downwelling. Theoretical models of mantle convection suggest that downwelling should occur in sheets or cylinders [16, 18], and it has been suggested that much of the downwelling is localized beneath the lowland planitiae [5,22] or beneath compressively deformed highlands [23]. The lowlands are also sites of pervasive plains volcanism [24], however, which would not be expected over regions of convective downwelling and lower than average upper mantle temperatures.

Many of the details required to associate particular regions on Venus with mantle flow patterns remain to be worked out. For instance, there is presently disagreement as to whether the volcanic plateau Lakshmi Planum in Ishtar Terra is located over a region of mantle downwelling, as might be suggested by the large-scale convergence implied by the formation of the bounding mountain belts [23,25], or over a region of mantle upwelling, as might be suggested by the pervasive volcanism [26,27] and aspects of the long-wavelength gravity anomaly [28]. As noted above, coronae have also been suggested as sites of mantle upwelling [4], although coronae typically have lesser dimensions (200-500 km) and are greater in number than the broad highland rises, and most coronae do not have a discernible gravity anomaly at present resolution. The relative ages of different coronae and the distribution of those coronae recently or even presently active have not been determined. If both broad rises and coronae are products of mantle upwelling, then multiple scales of mantle convection are indicated and the two forms of upwelling must presumably have different controlling geometries and buoyancy fluxes. A physical explanation for the different morphologies of the two classes of features has yet to be elucidated. Clearly, measurements by Magellan of high-resolution global gravity and further delineation of large-scale patterns of volcanism and tectonics and their temporal relationships will provide important new constraints on these issues.

References: [1] S.C. Solomon et al., *Science, 252*, 297, 1991; [2] V.L. Barsukov et al., *PLPSC 16th*, D378, 1986; [3] D.B. Campbell et al., *Science, 246*, 373, 1989; [4] A.A. Pronin and E.R. Stofan, *Icarus, 87*, 452, 1990; [5] R.J. Phillips et al., *Science, 252*, 651, 1991; [6] M.T. Zuber, *PLPSC 17th*, E541, 1987; [7] D. McKenzie et al., *JGR*, submitted, 1991; [8] S.E. Smrekar and R.J. Phillips, *EPSL*, in press, 1991; [9] R.J. Phillips et al., *Science, 212*, 879, 1981; [10] B.G. Bills et al., *JGR, 92*, 10335, 1987; [11] W.S. Kiefer et al., *GRL, 13*, 14, 1986; [12] R.J. Phillips, *JGR, 95*, 1301, 1990; [13] E.M. Robinson et al., *EPSL, 82*, 335, 1987; [14] W.M. Kaula, *Science, 247*, 1191, 1990; [15] R.J. Phillips, *GRL, 13*, 1141, 1986;[16] D. Bercovici et al., *Science, 244*, 950, 1989; [17] D.J. Stevenson et al., *Icarus, 54*, 466, 1983; [18] G. Schubert et al., *JGR, 95*, 14105, 1990; [19] B. Parsons and S. Daly, *JGR, 88*, 1129, 1983;[20] D. McKenzie and M.J. Bickle, *J. Petrol., 29*, 625, 1988; [21] G.E. McGill et al., *GRL, 8*,737, 1981; [22] M.T. Zuber, *GRL, 17*, 1369, 1990; [23] D.L. Bindschadler and E.M Parmentier, *JGR, 95*, 21329, 1990; [24] A.L. Sukhanov et al., *Map I-2059*, USGS, 1989; [25] W.S. Kiefer and B.H. Hager, *LPS, 20*, 520, 1989; [26] A.A. Pronin, *Geotectonics, 20*, 271, 1986; [27] A.T. Basilevsky, *Geotectonics, 20*, 282, 1986; [28] R.E. Grimm and R.J. Phillips, *JGR, 96*, 8305, 1990.

THE DEFORMATION BELTS OF LAVINIA PLANITIA. Steven W. Squyres, David G. Jankowski, Cornell University, Mark Simons, Sean C. Solomon, Bradford H. Hager, Massachusetts Institute of Technology, George E. McGill, University of Massachusetts

High-resolution radar images from the Magellan spacecraft have revealed the first details of the morphology of the Lavinia Planitia region of Venus. Several geologic units are present in the Lavinia region, defined using radar brightness, small-scale texture, characteristics and abundance of superposed structural features, and apparent relative ages. We divide the terrains of Lavinia Planitia into four broad groups: tessera terrains, textured terrains, regional plains, and digitate plains. Tessera occurs in Lavinia Planitia as scattered inliers surrounded and embayed by younger plains deposits. Textured terrain is common, and is as bright on the SAR image as tessera but does not exhibit the strong km-scale ridge and trough pattern of that unit. In places, it is possible to resolve a very regular fabric of bright lines at a scale of about 400 m in textured terrain, and it is this fabric that gives this material its distinctive appearance. Textured terrain occurs in two physiographic forms: 1) as plains that are significantly brighter than adjacent regional plains materials, and 2) as long, narrow ridges generally grouped together into ridge belts (see below). The areally dominant terrain type in Lavinia Planitia consists of moderately radar-dark to moderately radar-bright plains. Regional plains materials are most likely of volcanic origin, but morphologic forms resembling flows are rare. The two major sub-units of the regional plains are mottled plains composed in part of multiple overlapping shields, and dark plains on which individual flows are difficult to discern. Finally, digitate plains consist of complexes of digitate to locally lobate flows, many attaining lengths of hundreds of km.

Most of the plains areas of Lavinia contain long, narrow sinuous linear features that appear brighter than the background plains. These features are generally less than 1 km wide and a few tens of km long, although some reach widths of several km and lengths in excess of 100 km. Typical spacings range from several km to about 20 km, and locally up to 50 km. Where the topography of these features can be inferred from brightness variations in the SAR images they are clearly seen to have positive relief, although most simply appear as sinuous bright lineaments. We interpret these features to be compressional ridges, analogous to the wrinkle ridges commonly seen on the lunar maria. The wrinkle ridges of Lavinia Planitia show strong domainal preferred orientations, with regional trends that change very little over distances of hundreds of km. Wrinkle ridges appear to have formed in response to a temporally uniform stress field throughout the evolution of plains, because all plains units have them, including digitate plains.

Over much of western Lavinia are other bright lineaments that are geometrically distinct from the wrinkle ridges in that they are both longer and substantially straighter. In many instances they are too narrow to resolve as anything but a radar-bright line, but where they can be resolved they are seen to be narrow grooves. Lengths from 25 km to 75 km are common in some areas, while lengths of 150 to 200 km are common in others. A few grooves have lengths exceding 500 km. Spacings are also variable. Abutting relationships with wrinkle ridges suggest that some ridges are older than the grooves, some younger. We interpret these grooves to be narrow grabens. It is noteworthy that in all areas where grooves are present, their orientations are perpendicular to those of the wrinkle ridges. Thus, in a significant section of Lavinia Planitia is characterized by a distinctive "grid" pattern of orthogonal compressional and extensional features on the plains between the deformation belts.

The most obvious tectonic features of Lavinia Planitia are the prominent deformation belts that transect much of the surface. These belts take two very distinct forms, which we call *ridge belts* and *fracture belts*. The ridges that comprise ridge belts can vary considerably in width both from one to the next in a given belt and along the length of a single ridge. The maximum width observed is about 10 km, and more typical widths are a few km. Some ridges appear symmetric in cross-section, while others appear steeper on one flank than the other. A smooth, arch-like profile is most common, but some ridges show a narrow, rugged secondary ridge superimposed on the crest or on one flank, as is common for lunar wrinkle ridges. The ridges are typically rather sinuous, and commonly bifurcate and merge along strike, producing a complex anastomosing pattern. Some ridges appear to consist of textured terrain material, but in most places the evidence is not really definitive. Typical heights of individual ridges are 200-300 m. We interepret the ridge belts to be fold belts formed by belt-normal compression.

In contrast to ridge belts, fracture belts are dominated by a complex pattern of linear to

arcuate faults and fractures. Many faults appear singly, but others are paired to form grooves with widths ranging from a few km down to the resolution limit of the images. The faults commonly display complex anastomosing and crossing patterns that indicate repeated or progressive deformation. Where fracture belts change trend, or where belts bifurcate or merge, the pattern of faults is especially intricate. A noteworthy aspect of a few of the fracture belts is that in some parts of them two distinct scales of deformation are observed. Faults are spaced very closely (typically a few hundred m) almost everywhere they are present in fracture belts. However, in a few locales these closely-spaced faults are concentrated in bands of intense deformation that are separated by nearly undeformed materials. The bands typically are spaced 20-30 km apart. The relative elevations of the bands of intense and sparse deformation are uncertain at present. The fracturing in the bands might be the result of stretching across anticlinal crests, or alternatively might be regular concentrations of extensional deformation caused by a necking instability.

Magellan altimetry data have also provided the first detailed look at the topography of Lavinia Planitia. Overall, Lavinia is a broad, low plain, lying at a typical planetary radius of about 6050.5 km. A prominent characteristic of the altimetry of Lavinia is that both types of deformation belts are elevated significantly above the surrounding plains, with typical heights of hundreds of meters. The fracture belts in particular appear very rugged in the altimetric data.

There is some evidence for modest amounts of horizontal shear parallel to the axes of deformation belts. In one instance, an old set of plains grooves exhibits an S-shaped bend consistent with distributed left-lateral shear as it crosses the ridge belt. In another, a fracture belt exhibits a number of instances where paired faults form rhombohedral downdrops, in a manner similar to what is seen in terrestrial settings where extension is coupled with shear. We also have observed a series of apparent S-shaped minor folds along the lengths of individual ridges within a ridge belt, and distortion of well-developed penetrative fabric in textured terrain as the fabric impinges on a throughgoing, strongly lineated boundary of a ridge belt. In all of these cases, the amount of shear implied by the features observed is fairly minor.

The deformation belts in Lavinia did not all form contemporaneously. Instead, they show some significant variability in age, both with respect to the plains materials surrounding them and with respect to one another. A number of belts, particularly in western Lavinia, appear to deform the same material that constitutes the adjacent plains, with little or no subsequent volcanism. In the ridge belts, the transition from dark or mottled plains adjacent to the belt to the textured terrain of the belt is not necessarily a stratigraphic one in all cases; in some instances the texturing may simply result from the folding of the plains material. However, there are other very clear instances where belts are embayed and partially buried by lavas that postdate the belt deformation. Some clear crosscutting relationships are also observed that show that adjacent belts formed in a distinct sequence, rather than contemporaneously.

In some parts of Lavinia, deformation belt morphology appears to be related to the orientation of each belt with respect to the orthogonal grid of wrinkle ridges and grooves on the plains. Belts that whose orientations are closest to those of the plains grooves in their vicinity tend to be fracture belts, while those whose orientations are closest to those of local wrinkle ridges tend to be ridge belts. Even more notably, there are instances where a single belt changes from one trend to the other, and in so doing also changes tectonic style from one belt type to the other. There are also some belts where both ridges and fractures are common within the belt, and where the ridges lie parallel to local plains wrinkle ridges and the fractures lie orthogonal to them and parallel to local plains grooves.

A particularly important question is whether or the not ridge belts and fracture belts both owe their origin to a similar mechanism. Evidence suggesting that they may includes the gross geometric similarity of the two classes of belts (widths, positive topographic signatures, patterns traced across the plains) and the observation that in a few instances a single belt undergoes a transformation from ridge morpology to fracture morpology along its length. Similar morphologic transformations along the length of a belt have very recently been noted in Magellan images of the deformation belts of Atalanta Planitia as well. It is clear, however, that whatever the underlying cause of belt formation, the surface tectonic manifestations of ridge and fracture belts are markedly different.

Because of the gross similarities of both types of belts, and particularly because both are topographically raised, one reasonable working hypothesis is that both result from belt-normal

crustal shortening and thickening. In the case of the ridge belts, this argument is straightforward: the ridges are interpreted to be folds formed by ridge-normal compression. In the case of the fracture belts, however, the argument is really based only on the altimetry. All of the belts lie higher than the surrounding plains, and hence are attributed in this interpretation to a thickening, via belt-normal shortening, of the buoyant crust. While near-surface materials in the ridge belts have been deformed to produce folds, the same materials in fracture belts are intensely faulted in what appears to be a manifestation of near-surface extension, as could be produced by stretching of brittle surface materials across the crest of an arch-like uplift. The strongest argument that both belt types owe their origin to the same fundamental process may be that the single belts that exhibit both morphologies, depending on their local trend. We are pursuing the implications of this hypothesis in ongoing modeling work, but we note that other models for the origin of fracture belts may be worthy of consideration as well.

To summarize the tectonic evolution of the Lavinia region, we suggest that the regular grid of orthogonal wrinkle ridges and grooves on the plains formed in response to a regular stress field set up in the near-surface materials of the region. Then, at some depth below the surface, motions occurred that led to thickening of the crust along curvilinear belts. The orientations of these belts were not affected by the stresses responsible for the grid, and as a consequence the belts have irregular orientations unrelated to the orientation of the grid. Where a belt formed by crustal thickening lies perpendicular to the compressive axis of the grid, the surface manifestation of the deformation is folding. Where the thickened belt lies perpendicular to the extensional axis of the grid, one instead observes extensional faulting as materials are stretched across the uplift.

The scenario described above appears broadly consistent with the Magellan observations of Lavinia, but it raises many questions. Among them are:

(1) What process is responsible for the stress field that produced the regional grid, both here and elsewhere on Venus?

(2) What process is responsible for the crustal shortening that is inferred to have created the belts, and for the concentration of this shortening into belts?

(3) What do the dominant wavelengths of deformation within the belts indicate about the mechanical properties of the venusian crust?

(4) Can a self-consistent stress field description be found that accounts for the differing morphologies of ridge and fracture belts in terms of similar crustal thickening processes but differing near-surface stress states?

Geophysical modeling efforts are underway to address these questions, and preliminary results will be presented.

CORONA ANNULI: PLUME-RELATED MOUNTAIN BELT FORMATION ON VENUS, E.R. Stofan, Jet Propulsion Laboratory, D.L. Bindschadler and G. Schubert, Department of Earth and Space Sciences, UCLA

The annuli surrounding coronae on Venus are topographically raised regions characterized by extensional and compressional structures, and are analogous to more linear mountain belts identified on Venus. The spacing and morphology of compressional features within corona annuli, as well as the process of gravitational relaxation are similar to that seen in other, more linear mountainous regions on Venus. The annulae of some of the larger coronae such as Artemis are similar in elevation and extent to linear ridge and mountain belts. We analyze the morphology of corona annuli and pose some questions being investigated that may provide insight into the formation and modification of both corona annuli and linear mountain belts on Venus.

Coronae are circular to irregular structures on Venus surrounded by complex annuli of ridges and troughs [1-3]. Coronae range from 75-2600 km across, and most are topographically raised 0.5 to over 2 km above the surrounding region [4, 5]. Coronae are interpreted to be the surface manifestation of mantle plumes that have subsequently undergone gravitational relaxation [6, 7]. The great variety in corona morphology identified in Magellan data indicates that all of these features may not form by the same mechanism or combination of mechanisms. The annuli of coronae are characterized by a variety of tectonic features, usually some combination of troughs, compressional ridges, and lineaments of indeterminate origin. The majority of coronae mapped in Venera data appeared to have annuli dominated by compressional features [8]. The increased resolution of Magellan data indicates that some of the coronae identified in Venera data are also characterized by extension in their annuli, and that a far larger portion of the corona population is typified by annuli dominated by extensional faults and troughs. Variations in coronae annuli include simple graben as at Idem-Kuva Corona, fine-scale fractures as at Heng-o Corona, fractures and troughs on steep outer slopes as seen at Eithinoha Corona, graben on inner slopes of a topographic low as at Sarpanitum Corona, compressional features as at Sith Corona, a broad, relatively undeformed ridge as at Neyterkob Corona, or some combination of compressional and extensional features as at Artemis Corona. Ridges and/or troughs within a given annulus tend to be spaced 5-15 km apart. Annuli vary in width from about 10 to over 150 km across. The width of the annulus tends to increase somewhat with corona size. However, there is a great deal of variation in annulus width, with features of the same size having annuli that vary in width by a factor of ten. The largest annulus width measured to date, approximately 150 km, characterizes coronae that range in maximum width from 2600 km (Artemis) to 515 km (Bau Corona). The detailed relationship between the annulus and topography has not yet been determined. Some annuli are localized on sloping topography, others occur on relatively raised terrain, and some extend into the peripheral moat.

The annulus of corona is thought to form in the middle to late stages of corona evolution, following updoming of the surface and extensive volcanism as the plume approaches the surface. Bending of the lithosphere as the plume head flattens out and subsequent gravitational relaxation of topography are thought to account for extensional and compressional features identified in the annulus. Questions being addressed in the study of corona annuli and comparisons to more linear mountainous regions include: 1) What is the specific process that leads to compressional annulus formation and how does it differ from the apparently dominant process that leads to extension within annuli; 2) What is the relative importance of flexure in mountain belts and corona annuli and what are the sources of flexural loads?; 3) What is the specific relationship between compressional annulus structures and topography and

how does it compare to the relationships between compressional mountain belt structures and their topography, both on Earth and Venus?. Some of these questions can be addressed with Magellan image and altimetry data, while Magellan gravity data will provide insight into others.

References: 1) V.L. Barsukov *et al.*, *JGR*, 91, 378, 1986; 2) E.R.Stofan and J.W. Head, *Icarus*, *83*, 216, 1990; 3) S.C. Solomon *et al.*, *Science*, 1991; 4) E.R. Stofan *et al.*, submitted, *JGR*, 1991*a*; 5) S.W. Squyres *et al.*, submitted, *JGR*, 1991; 6) E.R. Stofan *et al.*, *JGR*, in press 1991*b*; 7) D.M. Janes *et al.*, submitted, *JGR*, 1991; 8) A.A. Pronin and E.R. Stofan, *Icarus*, *87*, 452, 1990.

TECTONIC SETTINGS OF THE MOUNTAIN BELTS OF VENUS; John Suppe and Chris Connors, Department of Geological and Geophysical Sciences, Princeton University, Princeton NJ 08544

As the high-resolution altimetry and imagery of Magellan reaches near global coverage it appears that the distribution of linear compressive mountain belts and rift systems on Venus—as on Earth—reflects a global pattern to the deformation of the lithosphere (Fig. 1)[1]. To the first approximation compressive mountain belts are concentrated in the northern hemisphere as a single high mountainous complex of Ishtar Terra about the size of Australia plus a low-elevation system of longitudinal fold belts, passing through the North pole and confined to the longitudes 150°-250°. In contrast, extensional tectonics is largely confined to the equatorial and southern latitudes as a near globe-encircling branching rift system. It is perhaps surprising that Venus can be fairly closely divided into extensional and compressional hemispheres separated by what might be called a *tectonic equator*, which is inclined about 40 degrees to the planetary equator. The pole to this tectonic equator is at about 63°, 44°N, within Leda Planitia. The linear fold belts and rift systems shown on Fig. 1 are simply the most obvious and apparently youngest deformational zones of substantial global extent. In addition there is significant distributed deformation of low intensity, especially wrinkle ridges, which typically display consistent orientations for thousands of kilometers. Furthermore some local compressive mountain belts exist associated with small subplates and local deformational environments, particularly within the globe-encircling rift system.

This global arrangement of young deformation on Venus can be described in a simple kinematic model[2] (Fig. 2) as an unearthly kind of plate tectonics consisting of two superplates, one that is growing and one that is shrinking. The shrinking superplate must be internally deforming as it converges toward the *tectonic pole*, whereas the growing plate need not deform. The shrinking superplate on Venus is currently the larger superplate, therefore it must be in extension south of the tectonic equator. Eventually, if large deformation and plate motion is occurring—which is not certain—the growing superplate will become the larger and only a minor portion of the planet will display compressive mountain belts.

This two-superplate model is a useful framework for introducing some of the key tectonic features of Venus. The southern, growing superplate displays relatively simple tectonics as might be expected: regionally systematic systems of wrinkle ridges within the plains, displaying at most a few percent shortening—except in a few places where they consolidate into small fold belts—and generally only one episode of deformation. Only a few very small areas of tessara exist, which are older highly polydeformed massifs. In contrast the northern superplate is much more tectonically complex, containing vast areas of tessara and polydeformed plains.

The fold-and-thrust belts are fairly similar to those on Earth: 100+ km wide and thousands of kms long with foredeep flexures, fault-bend folds 3-10 km wide above regionally extensive decollement, and flat high-plateau interiors. The fold belts exist at the margins of crustal blocks such as plateaus, tessera, and corona, and as ridge belts within the low plains. The regional topographic relief of fold belts—measured between the deformation toe and the flat crest—displays a remarkable roughly linear dependence on absolute elevation, ranging from 6 km for Maxwell Montes at an elevation of 10 km to a few hundred meters at the lowest planetary elevations (0 to –2 km). This phenomenon is proposed to be an effect of atmospheric temperature on the depth to the brittle-plastic transition along the decollement (Suppe and Connors, 1991).

---

[1]It should be noted that there is a general consensus that plate tectonics does not dominate heat transport on Venus (e.g. Kaula, 1990; Solomon and Head, 1991; Schubert, 1991; McGill, 1991), which has led some to conclude that plate tectonics does not exist, which does not necessarily follow.

[2]This model is based on mapping of the global Magellan data set (Fig. 1) plus thoughts about the super-continent cycle on Earth. During each episode of consolidation of supercontinents on Earth, compressive mountain belts were apparently confined to one hemisphere. It should also be noted that this two-superplate model of Venus is essentially an antisymmetric, non-steady version of Jason Morgan's two-plate model of Venus based on pre-Magellan altimetry (Morgan and Morgan, 1991).

TECTONIC SETTINGS OF MOUNTAIN BELTS OF VENUS: John Suppe & Chris Connors

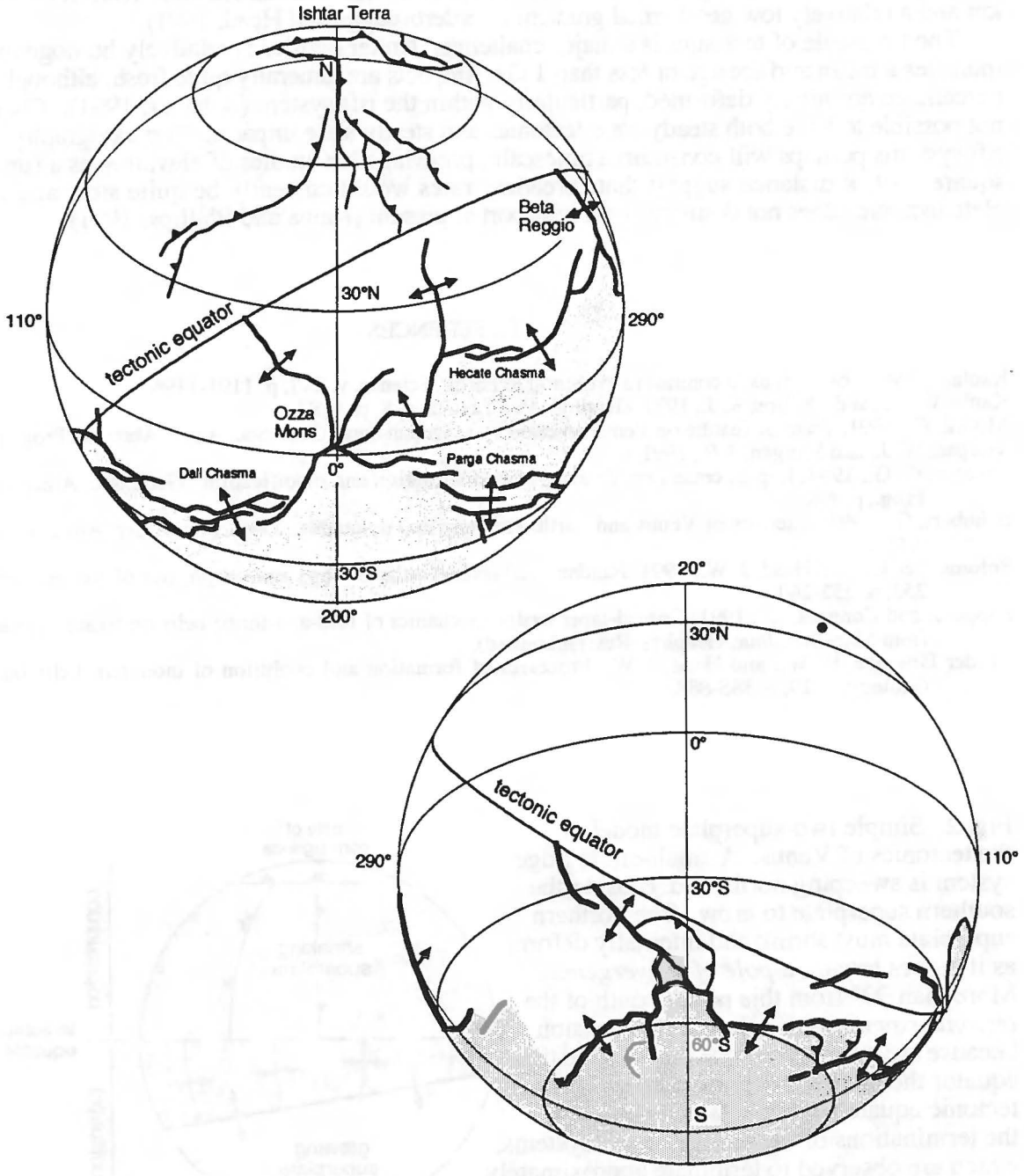

Fig. 1. Preliminary tectonic map of Venus showing young zones of linear deformation. Rift systems are shown in heavy black. Linear fold belts are shown in light barbed lines. Mapping to date suggests a branched, globe encircling rift system largely confined to one hemisphere (below the *tectonic equator* shown). Most major folded mountain belts are in the opposite hemisphere or are local zones of deformation associated with the rift system. Ishtar Terra in the north is the sole high-standing region of compressive mountain belts, reaching 11 km. The second major setting of compressive deformation is the low-relief longitudinal ridge belts in the low plains between the longitudes 150° and 250°. In addition to linear zones of deformation, substantial low intensity distributed deformation exists on Venus, particularly as wrinkle ridges. A simple unearthly two-plate model for Venus is shown in Fig. 2. The analogous growing superplate is shown in grey above.

TECTONIC SETTINGS OF MOUNTAIN BELTS OF VENUS; John Suppe & Chris Connors

The high mountainous region of Ishtar Terra is consistent with an isostatic root in excess of 45 km and a relatively low geothermal gradient (Vorderbruegge and Head, 1991).

The timescale of tectonics is a major challenge. Crater density is relatively homogeneous and indicates a mean surface age of less than 1 Ga. Impacts are generally quite fresh, although a small percentage are highly deformed, particularly within the rift system (Schaber, 1991). Clearly it is not possible to have both steady-state tectonics and steady-state impacts. The topography over the rift systems perhaps will constrain a timescale; pre-Magellan studies of elevation as a function of square-root of distance suggest that spreading rates would currently be quite slow and that any plate tectonics does not dominate heat transport at present (Kaula and Phillips, 1981).

REFERENCES

Kaula, W. M., 1990, Venus: a contrast in evolution to Earth. Science, v. 247, p. 1191-1196.

Kaula, W. M., and Phillips, R. J., 1981, Geophys. Res. Letters, v. 8, p. 1187

McGill, G., 1991, Tectonic feature on Venus revealed by Magellan data. Geol. Soc. Amer. Abstr. w/ Prog., p. A160.

Morgan, W. J., and Morgan, J. P., 1991, ms.

Schaber, G. G., 1991, Impact craters on Venus: global distribution and modification. Geol. Soc. Amer. Abstr. w/ Prog., p. A401.

Schubert, G., 1991, Interiors of Venus and Earth: structure and dynamics. Geol. Soc. Amer. Abstr. w/ Prog., p. A159.

Solomon, S. C., and Head, J. W., 1991, Fundamental issues in the geology and geophysics of Venus. Science, v. 252, p. 252-260.

Suppe, J. and Connors, C. , 1991, Critical-taper wedge mechanics of fold-and-thrust belts on Venus: initial results from Magellan. Jour. Geophys. Res. (submitted).

Vorder Bruegge, R. W., and Head, J. W., Processes of formation and evolution of mountain belts on Venus. Geology, v. 19, p. 885-888.

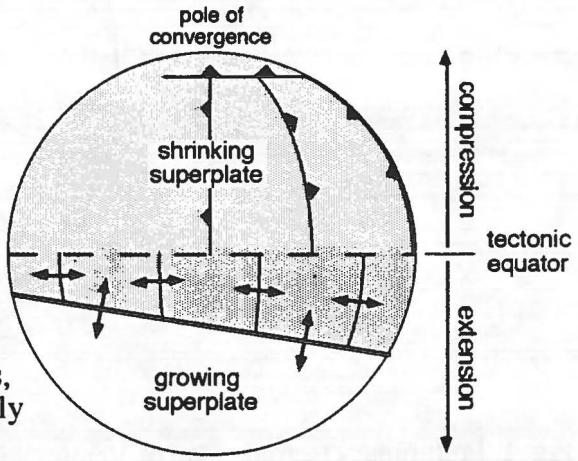

Fig. 2. Simple two-superplate model of the tectonics of Venus. A small-circle ridge system is sweeping northward, causing the southern superplate to grow. The northern superplate must shrink and internally deform as it moves toward a *pole of convergence.* More than 90° from this pole—south of the *tectonic equator*—the plate is in extension because arc radius is increasing. Above the equator the plate is in compression. The tectonic equator in Fig. 1 was located by the terminations of the secondary rift systems, which are observed to terminate approximately along a great circle—in agreement with this two-plate model.

FINITE AMPLITUDE, NON-NEWTONIAN FOLDING OF THE LITHOSPHERE ON VENUS AND EARTH; *M.T. Zuber*[1,2] and *E.M. Parmentier*[3], [1]Geodynamics Branch, NASA/Goddard Space Flight Center, Greenbelt, MD 20771; [2]Department of Earth and Planetary Sciences, The Johns Hopkins University, Baltimore, MD 21218; [3]Department of Geological Sciences, Brown University, Providence, RI 02912.

Radar images of the Ishtar Terra highland area of Venus have revealed the presence of parallel, regularly spaced, radar-bright and -dark lineations that trend along the axes of relatively narrow, elongated topographic highs [1,2,3]. These features have been interpreted as folds associated with mountain belts that formed in response to horizontal compression of the Venus lithosphere [1]. Using the assumption that the regular spacing of lineations represents the dominant wavelength of folding in a strength- or viscosity-stratified lithosphere, models have been developed to constrain thermomechanical properties of the lithosphere, such as effective elastic thickness [4], and crustal thickness and thermal gradient [5-7]. Two notable simplifications characterize these models: First, they assume simpler vertical viscosity distributions than are likely to describe the lithosphere. Second, the solutions are valid only for infinitesimal fold amplitudes (< < competent lithospheric layer thickness), and are thus not applicable at finite strains that may characterize highly-deformed fold belts. In order to develop a more realistic quantitative representation of lithospheric-sale shortening, we have constructed finite element models of a compressing medium that incorporate general vertical viscosity distributions and take into account non-Newtonian behavior of the lithosphere. With these models we address aspects of the structure and dynamical evolution of mountain belts on Venus and Earth.

We used a penalty function approach [8] to calculate deformation due to uniform horizontal shortening of an incompressible viscous medium with an arbitrary vertical viscosity distribution. Laboratory experiments on the strength of rock [*cf.* 9] extrapolated to appropriate temperatures and pressures indicate that the lithospheres of both Earth and Venus may contain regions of brittle deformation, characterized by a linear increase of strength with depth, and ductile deformation, characterized by an exponentially decreasing strength with depth. We thus defined a reference viscosity structure $\mu_o(z)$ corresponding to a typical strength envelope distribution (*cf.* Figure 2) using the expressions

$$\mu_o(z) = (\mu_1 - \mu_2)\frac{z}{z_{BD}} + \mu_2 \qquad z \geq z_{BD} \tag{1}$$

$$\mu_o(z) = \mu_1 e^{-z/d} \qquad z \leq z_{BD} \tag{2}$$

where μ_1 and μ_2 are the reference viscosities at the brittle-ductile transition and surface, respectively, z is relative depth, z_{BD} defines the relative thicknesses of the brittle and ductile regions, and d is the e-folding depth in the ductile region. The strain rate-dependent viscosity μ, with an assumed form

$$\mu = \mu_o \left[\frac{1}{\dot{\epsilon}_{II}}\right]^{1-\frac{1}{n}} \tag{3}$$

where $\dot{\epsilon}_{II}$ is the second invariant of the strain rate tensor and n is the power law exponent of stress, was estimated using an incremental procedure [10]. To approximate deformation in the brittle regime we invoked the assumption of perfect plasticity in which $n \to \infty$, while in the ductile creep regime we assumed $n = 3$.

The grid layout is schematically shown in Figure 1. The left boundary represents a symmetry plane in which the horizontal velocity, u, and shear stress, τ, vanish. The top boundary is stress free, and on the bottom boundary τ and the vertical velocity, w, vanish. On the right boundary τ vanishes and u is assigned a constant value. Values of u and the horizontal grid dimension were chosen so as to yield a normalized

FINITE AMPLITUDE FOLDING: Zuber M.T. and Parmentier E.M.

horizontal strain rate $\dot{\epsilon}_{xx}$ with a value of -1. Using this approach, the growth rates of folding determined from the finite element analysis could be directly compared to those from previous infinitesimal amplitude analytical solutions [5,6]. In the analytical solutions the dimensionless rate of fold growth q is expressed

$$q = \frac{\ln \frac{\Delta}{\Delta_o}}{\dot{\epsilon}_{xx} t} - 1 \qquad (4)$$

where Δ_o is the amplitude of initial random interface perturbations and Δ is the fold amplitude at time t. In the finite element models q is determined from the slope of the relationship between the natural log of the rms amplitude of deformation, and the horizontal strain $\dot{\epsilon}_{xx} t$.

Figure 2 shows estimates of q for three vertical viscosity distributions with fixed thickness and viscosity structure in the brittle layer and different values of d for the ductile layer. In each case q exceeds the critical value of one, which indicates that lithospheres with all of these viscosity distributions will develop folds when horizontally compressed. As for the infinitesimal amplitude solutions [5,6], the rate of fold amplitude growth is greater for smaller d. Also note that with decreasing d, q progressively decreases with increasing $\dot{\epsilon}_{xx} t$, indicating that folds will grow increasingly slowly at finite strains.

In infinitesimal amplitude solutions, folding instabilities are driven by discontinuities in vertical viscosity at the surface or at interfaces between layers [*e.g.* 11]. However, Figure 2 demonstrates that a medium with a vertical viscosity distribution that is everywhere continuous and that approximates the probable vertical distribution of strength in the lithosphere is also unstable with respect to folding. Hence, discontinuities in vertical viscosity, either within the lithosphere or at the surface, are not required for the development of folds. It is interesting to note that the growth rates obtained in Figure 2 are nearly identical to those predicted if the brittle layer were instead characterized by a uniform viscosity μ_1. This indicates that the rate of fold growth in a medium with a distributed driving force associated with a continuous vertical viscosity distribution can be adequately estimated from a medium with a discrete viscosity jump at the surface. However, calculation of the perturbed velocity field that characterizes the style of deformation should be based on the detailed viscosity structure.

The solutions in Figure 2 assume no lateral viscosity variations. However, spatial variations in lithospheric thickness might be expected on Earth or Venus due to thermal, compositional or mechanical heterogeneities. Simple solutions for compression of a non-Newtonian viscous lithospheric layer with a small thickness variation show significant stress supported topography that may explain salient morphologic features of certain mountain belts [12]. Similar models adapted to consider finite lithospheric thickness variations may be relevant to the large-scale topographic expression of structures on Earth and Venus, such as the Himalayas that border the Tibetan Plateau, and Vesta Rupes and Akna and Freyja Montes that surround Lakshmi Planum.

References: [1]Campbell, D.B. et al., *Science, 221,* 644-647, 1983. [2]Barsukov, V.L. et al., *J. Geophys. Res., 91,* D378-D398, 1986. [3]Solomon, S.C. et al., *Science, 252,* 297-312, 1991. [4]Solomon, S.C., and J.W. Head, *J. Geophys. Res., 89,* 6885-6897, 1984. [5]Zuber, M.T., *J. Geophys. Res., 92,* E541-E551, 1987. [6]Zuber, M.T., and E.M. Parmentier, *Icarus, 85,* 290-308, 1990. [7]Banerdt, W.B., and M.P. Golombek, *J. Geophys. Res., 93,* 4759-4772, 1988. [8]Bathe, K.-J., *Finite Element Procedures in Engineering Analysis,* 735 pp., Prentice-Hall, Inc. Englewood Cliffs, 1982. [9]Brace, W.F., and D.L. Kohlstedt, *J. Geophys. Res., 85,* 6248-6252, 1980. [10]Desai, C.S., and Abel, J.F., *Introduction to the Finite Element Method,* 477 pp., Van Nostrand Reinhold, New York, 1972. [11]Fletcher, R.C., *Am. Jour. Sci., 274,* 1029-1043, 1974. [12]Parmentier, E.M., *Lunar Planet. Sci. Conf., XVII,* 648-649, 1986.

FINITE AMPLITUDE FOLDING: Zuber M.T. and Parmentier E.M.

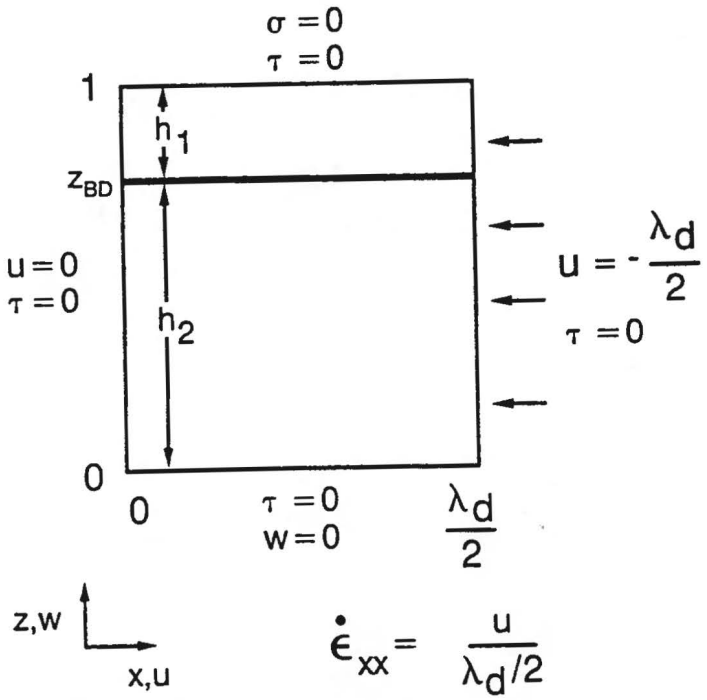

Figure 1. Geometry and boundary conditions for the non-Newtonian finite element folding problem.

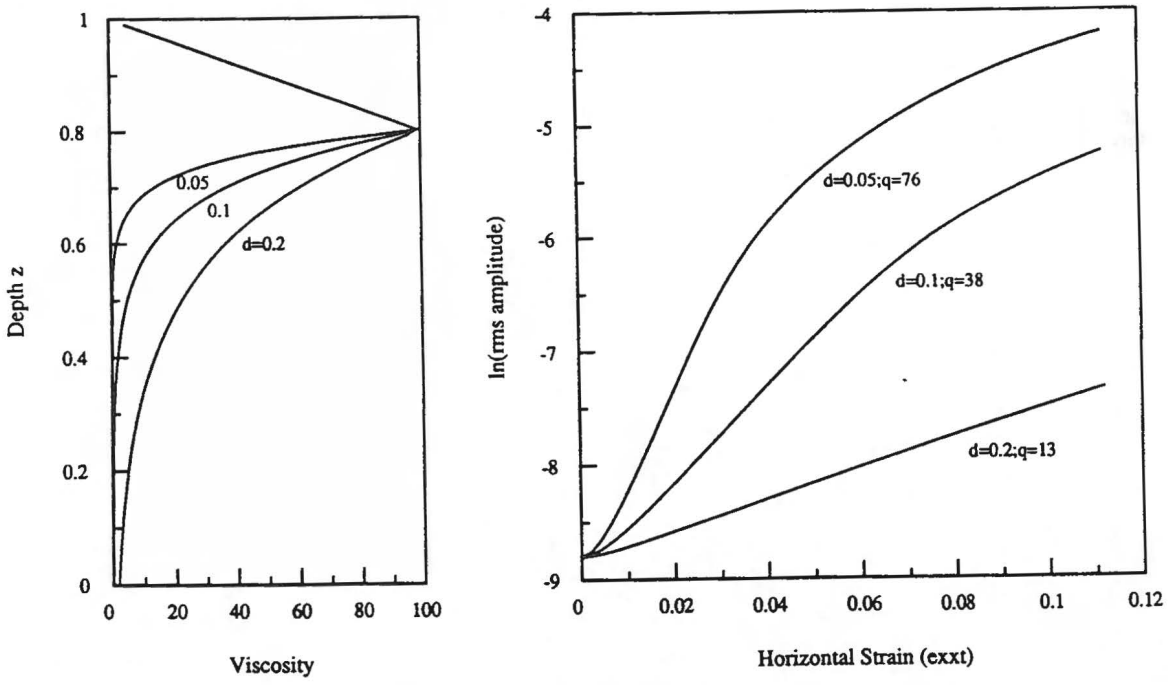

Figure 2. Vertical viscosity structures (left) and associated relationships between ln(rms amplitude) and mean horizontal strain. The slopes of the lines on the right give the growth rates of folding, q. Parameter values for this calculation are $\mu_1=100$, $\mu_2=0$, $z_{int}=0.8$, $n_1=100$, and $n_2=3$. Values of q listed represent those at small strains, where the slopes, and growth rates, are greatest. For $d=0.1$ and 0.05, the slopes of the lines decrease at larger strains, indicating that the rate of fold amplitude growth also decreases.